GMRT an Overview

Giant Metrewave Radio Telescope (GMRT), located 80 km north of Pune in India, is the world's largest radio telescope working at metre wavelengths. It is operated by the National Centre for Radio Astrophysics, a part of the Tata Institute of Fundamental Research, Bombay. In the form of GMRT, NCRA (National Center for Radio Astrophysics, TIFR) holds the facility for radio astronomical research using the meter wavelengths range of the radio spectrum. It consists of 30 fully steerable giant parabolic dishes of 45m diameter each spread over distances of up to 25 km. GMRT is one of the most challenging experimental program in basic sciences undertaken by Indian scientists and engineers.

The site for GMRT was selected after an extensive search in many parts of India, considering several important criteria such as low radio frequency interference, availability of good communication, vicinity of industrial, educational and other infrastructure and, a geographical latitude sufficiently north of the geomagnetic equator in order to have a reasonably quiet ionosphere and yet be able to observe a good part of the southern sky as well.

Meter Wavelength Observation – a challenge

The Astronomical Bodies and Events can be fully studied if we can view the universe with different wavelengths and compare the records all together. Since the universe seems to be different at different wavelengths.

But from the technical and practical point of view the universe at higher frequencies can be viewed easily as it is easier to develop a radio telescope for high frequencies, but the most challenging work was to develop a telescope which can work at low frequencies or more specifically Radio Frequencies because this is the range of frequencies in which maximum noise lies. In aboard, countries like USA, the RF Noise level is too high, no other country had taken an initiative to develop such a system working at this frequency range. The RF noise level being comparatively low in India, holds the opportunity to pick up this challenging project of GMRT working at Radio frequencies.

Hence, the meter wavelength part of the radio spectrum has been particularly chosen for study with GMRT because artificial radio interference is considerably lower in this region of the spectrum in India. Although there are many outstanding astrophysics problems which are best studied at meter wavelengths, there has, so far, been no large facility anywhere in the world to exploit this part of the spectrum for astrophysical research. The Astronomical bodies that can be best studied at meter wavelengths through GMRT are –

Pulsars, Sun, Jupiter Radio Bursts, Hydrogen Lines, Milky way and other nearby Galaxies.

Technical Information

The number and configuration of the dishes is optimized to meet the principal astrophysical objectives which require sensitivity at high angular resolution as well as ability to image radio emission from diffuse extended

GMRT ARRAY CONFIGURATION
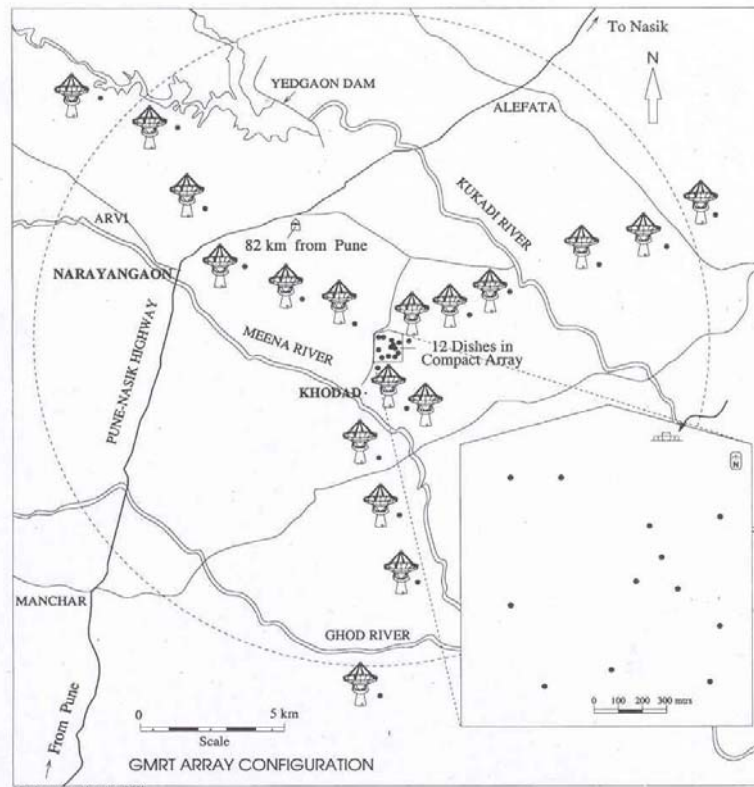
regions. Fourteen of the thirty dishes are located more or less randomly in a compact central array in a region of about 1 sq km. The remaining sixteen dishes are spread out along the 3 arms of an approximately `Y'-shaped configuration over a much larger region, with the longest interferometric baseline of about 25 km. The multiplication or correlation of radio signals from all the 435 possible pairs of antennas or interferometers over several hours thus enables radio images of celestial objects to be synthesized with a resolution equivalent to that obtainable with a single gigantic dish 25 km in diameter. The GMRT array operates in six frequency bands centered on 50, 150, 233, 327, 610 and 1000-1420 MHz . All these feeds provide dual polarization outputs. The highest angular resolution achievable ranges from about 60 arc-secs at the lowest frequencies to about 2 arc-secs at 1.4 GHz.

The construction of 30 large dishes at a relatively small cost has been possible due to an important technological breakthrough achieved by Indian Scientists and Engineers in the design of light-weight, low-cost dishes. The design is

based on what is being called the `**SMART'** concept - for Stretch **M**esh Attached to **R**ope **T**russes.

The dish has been made light-weight and of low solidity by replacing the conventional back-up structure by a series of rope trusses (made of thin stainless steel wire ropes) stretched between 16 parabolic frames made of tubular steel. The wire ropes are tensioned suitably to make a mosaic of plane facets approximating a parabolic surface. A light-weight thin wire mesh (made of 0.55 mm diameter stainless steel wire) with a grid size varying from 10 X 10 mm in the central part of the dish to 20 X 20 mm in the outer parts, stretched over the rope truss facets forms the reflecting surface of the dish. The low-solidity design cuts down the wind forces by a large factor and is particularly suited to Indian conditions where there is no snowfall in the plains. The overall wind forces and the resulting torques for a 45-m GMRT dish are similar to those for only a 22-m dish of conventional design, thus resulting in substantial savings in cost.

The dish is connected to a `cradle' which is supported by two elevation bearings on a yoke placed on a 3.6 m diameter slewing-ring bearing secured on the top of a 15 meter high concrete tower. The weight of the disk is about 80 tonnes and the counter-weight is about 40 tonnes. The dishes have alt-azimuth mount.

Receiver System

The GMRT currently operates at 5 different frequencies ranging from 150 MHz to 1420 MHz. Some antennas have been equipped with receivers which work up to 1750 MHz. Above this frequency range however, the antenna performance degrades rapidly both because the reflectivity of the mesh falls and also because of the rapidly increasing aperture phase errors because of the deviations of the plane mesh facets from a true parabola. A 50 MHz receiver system is also planned. Table below gives the relevant system parameters at the nominal center frequency of the different operating frequencies of the GMRT.

Table 18.1: *System parameters of the GMRT*

System Properties				in MHz		
	50	153	233	327	610	1420
Primary beam (degree)		3.8	2.5	1.8	0.9	0.4×(1400/f)
Synthesized beam						

Full array (arc sec)		20	13	09	05	02
Central array (arc min)		7.0	4.5	3.2	1.7	0.7
System temperature (K)						
(1) $T_{receiver}$		144	55	50	60	40
(including cable losses)						
(2) $T_{ground} = T_{mesh} + T_{spilover}$		30	23	18	22	32
(3) T_{sky}		308	99	40	10	4
Total T_{sys}		482	177	108	92	76
$= T_{sky} + T_{receiver} + T_{ground}$						
Gain of an antenna (K/Jy)		0.33	0.33	0.32	0.32	0.22
RMS noise in image* (μJy)		46	17	10	09	13

*For assumed bandwidth of 16 MHz, integration of 10 hours and natural weighting (theoretical).

The GMRT feeds, (except for the 1420 feed), are circularly polarized. The circular polarization is achieved by means of a polarization hybrid inserted between the feeds and the RF amplifiers. No polarization hybrid was inserted for the 1420 MHz feed, in order to keep the system temperature low. None of the receivers are cooled, i.e. they all operate at the ambient temperature. The feeds are mounted on four faces of a feed turret placed at the focus of the antenna. The feed turret can be rotated to make any given feed point to the vertex of the antenna. The feed on one face of the turret is a dual frequency feed, i.e. it works at both 233 MHz as well as 610 MHz.

After the first RF amplifier, the signals from all the feeds are fed to a common second stage amplifier (this amplifier has an input select switch allowing the user to choose which RF amplifier's signal is to be selected), and then converted to IF. Each polarization is converted to a different IF frequency, and then fed to a laser-diode. The optical signals generated by the laser-diode are transmitted to a central electronics building (CEB) by fibre optic cables. At the central electronic building, they are converted back into electrical signals by a photo-diode, converted to baseband frequency by another set of mixers, and then fed into a suitable digital backend. Control and telemetry signals are also transported to and from the antenna by on the fibre-optic communication system. Each antenna has two separate fibres for the uplink and downlink.

Digital Backends

There are a variety of digital backend available at the GMRT. The principle backend used for interferometric observations is a 32 MHz wide FX correlator. The FX correlator produces a maximum of 256 spectral channels for each of two polarizations for each baseline. The integration time can be as short as 128 ms, although in practice 2 sec is generally the shortest integration time that is used. The FX correlator itself consists of two 16 MHz wide blocks, which are run in parallel to provide a total instantaneous observing bandwidth of 32 MHz. For spectral line observations, where fine resolution may be necessary, the total bandwidth can be selected to be less than 32 MHz. The available bandwidths range from 32 MHz to 64 kHz in steps of 2. The maximum number of spectral channels however remains fixed at 256, regardless of the total observing bandwidth. The GMRT correlator can measure all four Stokes parameters; however this mode has not yet been enabled. In the full polar mode, the maximum number of spectral channels available is 128. Dual frequency observations are also possible at 233 and 610 MHz, however in this case; only one polarization can be measured at each frequency. The array can be split into sub-arrays, each of which can have its own frequency settings and target source. The correlator is controlled using a distributed control system, and the data acquisition is also distributed. The correlator output, i.e. the raw visibilities are recorded in a GMRT specific format, called the ``LTA'' format. Programmes are available for the inspection, display and calibration of LTA files, as well as for the conversion of LTA files to FITS. The first block of the GMRT pulsar receiver is the GMRT Array Combiner (GAC) which can combine the signals from the user-selected antennas (up to a maximum of 30) for both incoherent and coherent array operations. The input signals to the GAC are the outputs of the Fourier Transform stage of the GMRT correlator, consisting of 256 spectral channels across the bandwidth being used, for each of the two polarizations from each antenna. The GAC gives independent outputs for the incoherent and coherent array summed signals, for each of two polarizations. For nominal, full bandwidth mode of operation, the sampling interval at the output of the GAC is 16μsec.

Different back-end systems are attached to the GAC for processing the incoherent and coherent array outputs. The incoherent array DSP processor takes the corresponding GAC output signals and can integrate the data to a desired sampling rate (in powers of 2 times 16μsec). It gives the option of acquiring either one of the polarizations or the sum of both. It can also collapse adjacent frequency channels, giving a slower net data rate at the cost of reduced spectral resolution. The data is recorded on the disk of the main computer system.

The coherent array DSP processor takes the dual polarization, coherent (voltage sum) output of the GAC and can produce an output which gives 4 terms - the intensities for each polarization and the real and imaginary parts of the cross product - from which the complete Stokes parameters can be reconstructed. This hardware can be programmed to give a sub-set of the total intensity terms for each polarization or the sum of these two. The minimum sampling interval for this data is 32μsec, as two adjacent time samples are added in the hardware. Further reintegration (in powers of 2) can be programmed for this receiver. The final data is recorded on the disk of the main computer system.

There is another independent full polarimetric back-end system that is attached to the GAC. This receiver produces the final Stokes parameters, I,Q,U & V. However, due to a limitation of the final output data rate from this system, it it cannot dump full spectral resolution data at fast sampling rates. Hence, for pulsar mode observations the user needs to opt for online dedispersion or gating or folding before recording the data (there is also a online spectral averaging facility for non-pulsar mode observations).
In addition, there is a search pre-processor back-end attached to the incoherent array output of the GAC. This unit gives 1-bit data, after subtracting the running mean, for each of the 256 spectral channels. Either one of the polarizations or the sum of both can be obtained.

Most sub-systems of the pulsar receiver can be configured and controlled with an easy to use graphical user interface that runs on the main computer system. For pulsar observations, since it is advisable to switch off the automatic level controllers at the IF and baseband systems, the power levels from each antenna are individually adjusted to ensure proper operating levels at the input to the correlator. The format for the binary output data is peculiar to the GMRT pulsar receiver. Simple programs to read the data files and display the raw data - including facilities for dedispersion and folding - are available at the observatory and can be used for first order data quality checks, both for the incoherent mode and coherent mode systems.

****

1.1. **Antenna:**

An antenna can be defined as a "means for radiating or receiving radio waves." In other words the antenna is the transitional structure between free space and guiding device. Regardless of the type, all antennas have the same basic principle that radiation is produced by accelerated charge. The basic equation of radiation may simply be expressed as

$$IL=Qv$$

where

I= time changing current, As^{-1}

L= length of the current element, m

Q= charge, C

v=time charge of velocity (acceleration), ms^{-2}

The transmitting antenna is a region of transition from a guided wave on a transmission line to a free space wave. The receiving antenna is a region of transition from a free space wave to a guided wave on a transmission line. Thus an antenna may also be regarded as a transition device or transducer between a guided wave and a free space wave or vice-versa.

From the circuit point of view, the antenna to the transmission lines as a resistance R_r, known as radiation resistance which is not related to the resistance in the antenna itself but is resistance coupled from space to the antenna terminals.

In the transmitting case, the radiated power is absorbed by distant objects such as trees, buildings, the ground, the sky and other antennas. In the receiving case passive radiations from distant objects or active radiations from other antennas raises the temperature of the radiation resistance. This temperature has nothing to do with the physical temperature of the antenna but is related to temperature of distant objects that the antenna is looking at.

To describe the performance of the antenna, it is necessary to describe various parameters associated with antenna.

1.2 Radiation Pattern or Antenna Pattern:

Radiation pattern of an antenna is defined as the mathematical function or a graphical representation of the radiation properties of the antenna as a function of space coordinates. In most of the cases, the radiation pattern is determined in the far field region and is represented as a function of space coordinates. Radiation properties include power flux density, radiation intensity, field strength, directivity phase or polarization. The radiation property of most concern is the two or three dimensional spatial distribution of radiated energy as a function of observer's position along a path or surface of constant radius. A trace of received power at a constant radius is called power pattern. On the other hand, a graph of the spatial variation of the electric or magnetic field along a constant radius is called amplitude field pattern.
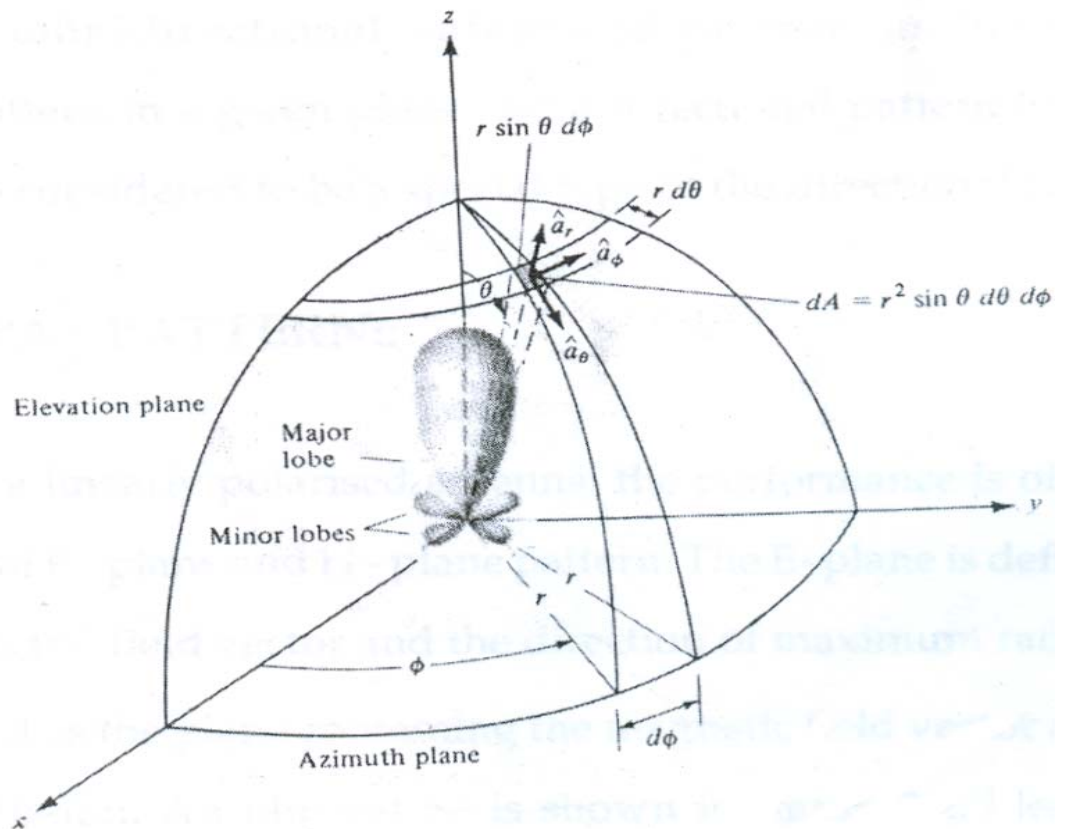
Fig 1: Co-ordinate system for antenna analysis

1.3 Isotropic, Directional and Omni-directional Pattern:

A hypothetical lossless antenna having equal radiation in all direction is called an isotropic antenna. However such a case is ideal, not realizable in practice and often taken as a reference for expressing the directive properties of the actual antenna.

A directional antenna is defined as the antenna having the property of radiating or receiving electromagnetic waves more effectively in some direction than the others. This term is usually applied to an antenna whose directivity is significantly greater than the half-wave dipole.

An omnidirectional antenna is defined as having essentially non-directional pattern in a given plane and a directional pattern in any orthogonal plane. It may also consider being a special type of the directional pattern.

1.4 Principal Pattern

For a linearly polarized antenna, the performance is often described in terms of its principal E-plane and H-plane pattern. The E-plane is defined as the plane containing the electric field vector and the direction of maximum radiation and the H-plane is defined as the plane containing the magnetic field vector and the direction of maximum radiation. An illustration is shown in figure 2. Here, the x-z plane (elevation plane; $\varphi=0$) is the E-plane and x-y plane (azimuthal plane; $\theta=\pi/2$) is the H-plane.
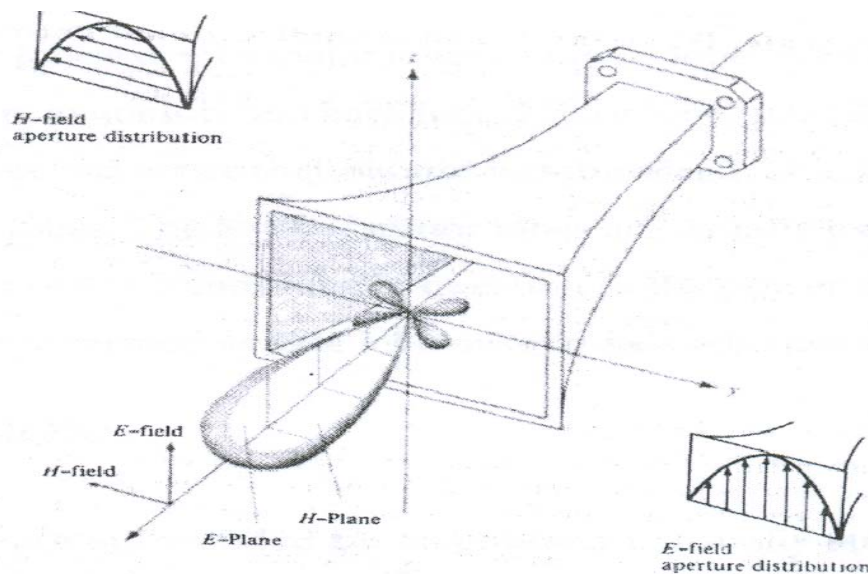
Fig2: Principal E-pattern and H-pattern

1.5 Radiation Pattern Lobe:

A radiation lobe is a portion of radiation pattern bounded by relatively weak radiation intensity. Radiation lobes are classified as major or main, minor, side and back lobes.

A major lobe is defined as the lobe containing the direction of maximum radiation. Any other lobe except a major lobe is the minor lobe. A lobe whose axis makes an angle 180° with the major lobe is a back lobe. Minor lobes usually represent radiation in undesired direction and hence they should be minimized. Side lobes are usually the largest of the minor lobes. The level of minor lobes is usually expressed as the ratio of the power density of the minor lobe in question to the power density of the major lobe. This ratio is often termed as side lobe ratio or side lobe level.
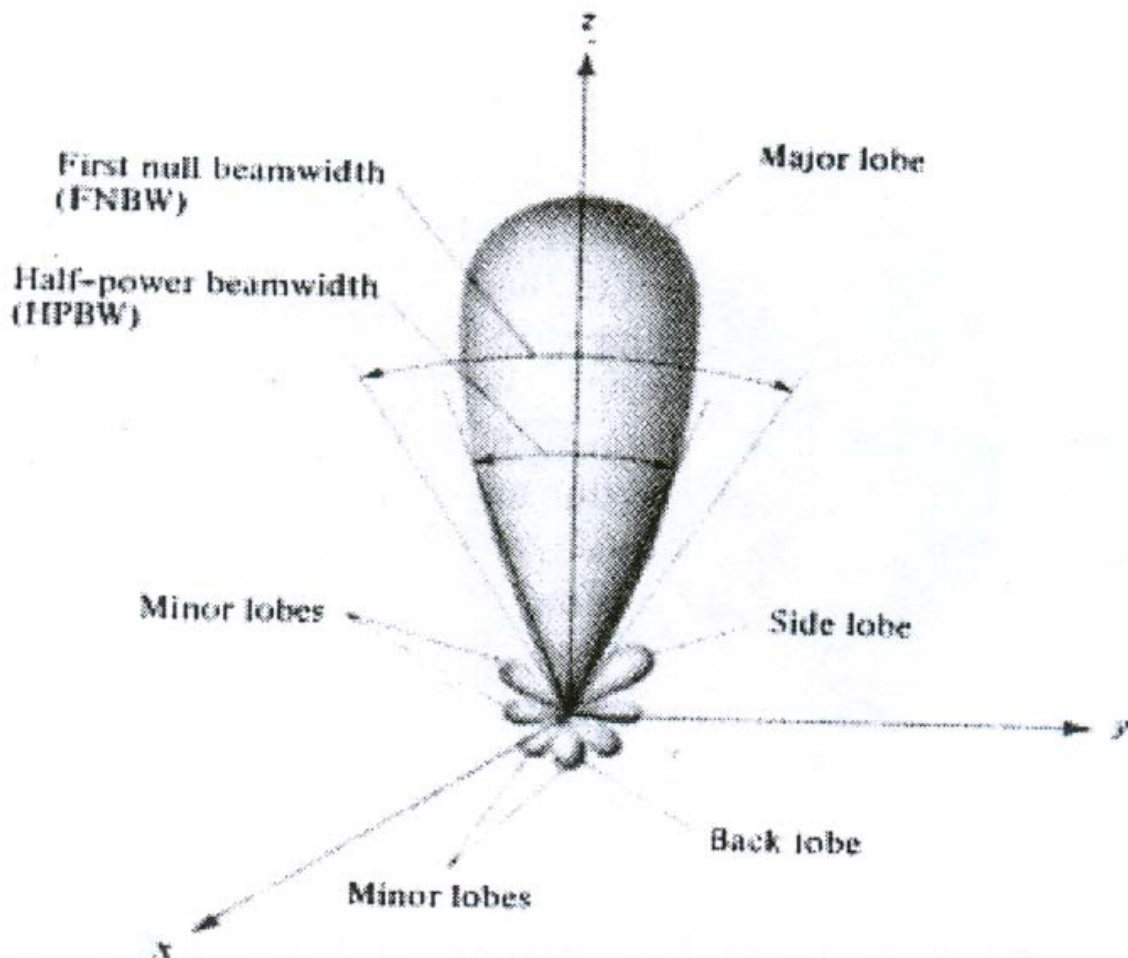
Fig3: Radiation lobes

1.6 Field Regions:

The space surrounded by an antenna is usually subdivided into three regions,

a) Reactive near field region

b) Radiating near field region(Fresnel)

c) Far field region(Fraunhofer)
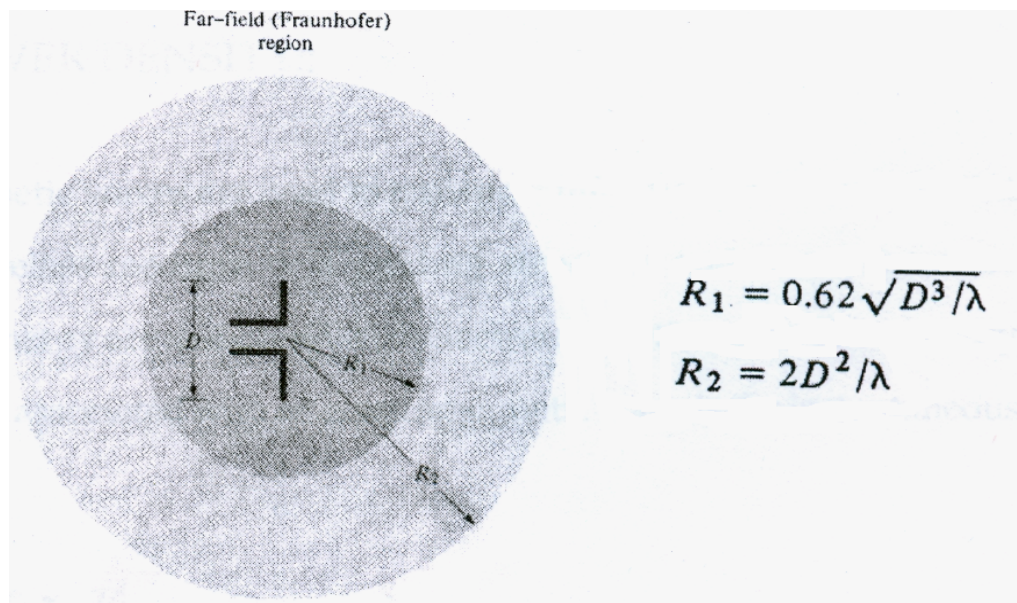
Fig4: Field regions of an antenna

Reactive near field region is defined as that portion of the near field region immediately surrounding the antenna wherein the reactive field predominates. For most antennas, this region is commonly taken to exist at a distance R< 0.62

$\overline{}$ where the wavelength is and D is the largest dimension of the antenna.

Radiating near field is defined as that region of the field of an antenna between the reactive near field region and the far field region wherein the angular field distribution is dependent upon the distance from the antenna. The

radiating near field region is taken to exists to a distance R such that 0.62 $\overline{}$

<R<$\overline{}$. If maximum dimension of the antenna is not large compared to wavelength or if the maximum overall dimension is very small compared to wavelength then this region may not exist.

Far field region is defined as that region of the field where the angular field distribution is independent of the distance from the antenna. The far field region is taken to exist at distances R<$\frac{2D^2}{\lambda}$.

1.7 Radiation Power Density:

Electromagnetic waves are used to transport information from one point to another through a wireless medium or a guiding structure and hence it can be assumed that power and energy are associated with electromagnetic wave. The quantity used to describe the power associated with an electromagnetic wave is the instantaneous Poynting vector given by

W= E × H

where

W= Instantaneous Poynting vector (w/m^2)

E= Instantaneous electric field intensity

H= Instantaneous magnetic field intensity

Since the Poynting vector is a power crossing a closed surface can be obtained by integrating the normal component of Poynting vector over the entire surface. Mathematically,

P= $\iint W.dS = \iint W.n\, da$

Where

P= Instantaneous total power (W)

n= unit vector normal to the surface

da= infinitesimal area of the closed surface (m^2)

The average power radiated by an antenna (radiate power) can be written by,

$P_{rad} = P_{av} = \iint W_{rad}.ds = \iint W_{av}.n\, da$

$= \frac{1}{2} \iint Re\, (E \times H^*).dS$

For an isotropic radiator(ideal case)as the source radiates in all direction Poynting vector have only radiated component and will not be a function of the spherical coordinate angles θ and φ. Hence total power radiated

$P_{rad}= W_o .dS = 4\pi r^2 W_o$

And the power density

$W_o = a_r W_o = a_r \left(\frac{P_{rad}}{4\pi r^2}\right) (W/m^2)$

which is uniformly distributed over a surface of radius r.

1.8 Radiation Intensity:

Radiation intensity is defined as the power radiated from an antenna per unit solid angle. It is a far field parameter and mathematically it can be given as

$U = r^2 W_{rad}$

where ,

U is the radiation intensity (W/unit solid angle)

W_{rad} is the radiation density (W/m²)

r is the distance in meter.

The total power radiated in this case can be given by,

$P_{rad}= \iint U \, d\Omega = \int_0^{2\pi} \int_0^{\pi} U \sin\theta \, d\theta \, d\phi$

where,

$d\Omega$ = element of solid angle = $\sin\theta \, d\theta \, d$

For isotropic source U is independent of θ and

$\therefore P_{rad}= \iint_{\Omega} U_o \, d\Omega = U_o \iint_{\Omega} d\Omega = 4\pi U_o$

$\therefore U_o = \frac{P_{rad}}{4\pi}$

1.9 Antenna Temperature:

In the transmitting case, radiated power is power is absorbed by distant objects, trees, buildings, the ground, the sky and other antennas. In the receiving case, passive radiations from distant objects or active radiations from other antennas raises the apparent temperature of the antenna. From a lossless antenna this temperature has nothing to do with the physical temperature of the antenna itself, but is related to temperature of distant objects to which the antenna is looking at.

Every object having physical temperature above absolute zero radiates energy. The amount of energy radiated is usually represented by an equivalent temperature T_B called brightness temperature and is defined as

$$T_B(\theta, \phi) = \epsilon (\theta, \phi) T_m = (1 - |\Gamma|^2) T_m$$

Where

T_B = brightness temperature (K)

ϵ = emissivity (dimensionless)

T_m = molecular (physical) temperature (K)

$\Gamma (\theta, \phi)$ = reflection coefficient of the surface of polarization of the wave

Since $0 \leq \epsilon \leq 1$, the maximum value of T_B is equal to T_m. Usually emissivity is a function of the frequency of operation.

Brightness temperature emitted by different sources is intercepted by antennas and appears at the terminals as an antenna temperature. It can be given as

$$T_A = \frac{\iint_0^{2\pi} \iint_0^{\pi} T_B(\theta,\phi) G(\theta,\phi) \sin\theta \, d\theta \, d\phi}{\iint_0^{2\pi} \iint_0^{\pi} G(\theta,\phi) \sin\theta \, d\theta \, d\phi}$$

where

T_A = antenna temperature (effective noise temperature of the antenna radiation resistance)

$G (\theta, \phi)$ = gain (power) pattern of the antenna

Assuming that there is no loss or contribution between antenna and receiver, the noise power transferred to the antenna is given as

$$P_r = kT_A\Delta f$$

Where

P_r = antenna noise power (W)

K = Boltzmann constant (1.38×10^{-23} J/K)

Δf = bandwidth (Hz)

If the antenna and the transmission line are maintained at certain temperature and the transmission line is lossy then the antenna temperature at the receiver terminals in modified from can be given as

$$T_a = T_A e^{-2\alpha l} + T_{AP}e^{-2\alpha l} + T_o(1-e^{-2\alpha l})$$

where

$$T_{AP} = \left(\frac{1}{e_A} - 1\right)T_P$$

T_a = antenna temperature at the receiver terminals (K)

T_{AP} = antenna temperature at the antenna terminals due to physical temperature

T_P = antenna physical temperature (K)

α = attenuation coefficient of transmission line (Np/m)

e_A = thermal efficiency of antenna (dimensionless)

T_o = physical temperature of the transmission line (K)

In that case the antenna noise power must also be written in modified form as

$$P_r = k\, T_a\Delta f$$
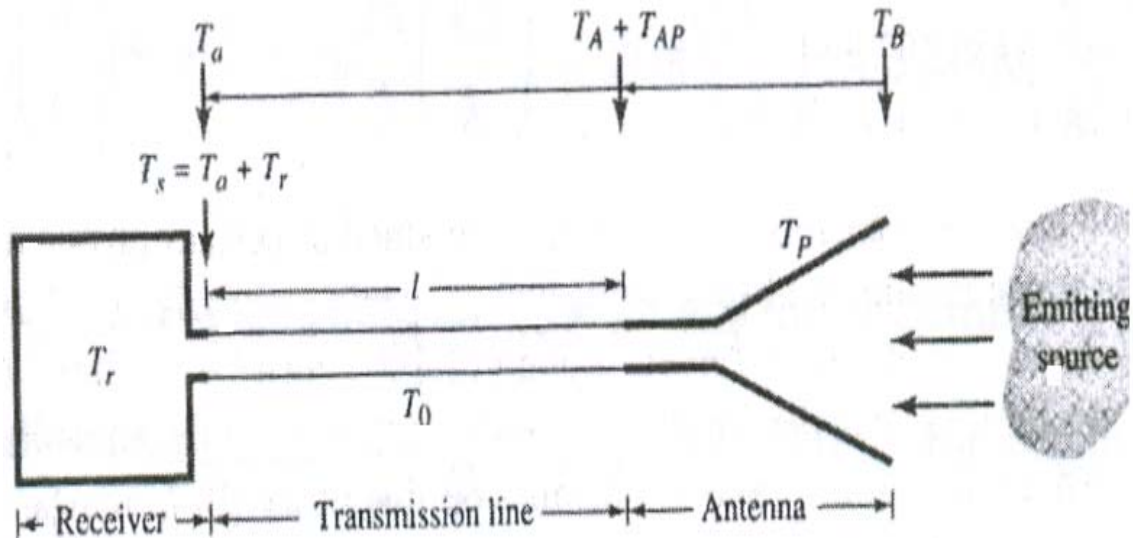
Fig5: Antenna transmission line and receiver arrangement

If the receiver itself has a certain noise temperature T_r, the system noise temperature at the terminals is given as,

$$P_s = k\,(T_a + T_r)\,\Delta f = kT_s\Delta f$$

where

T_r = antenna noise temperature (at receiver terminals)

$T_s = T_a + T_r$ = effective system noise temperature (at receiver terminals)

1.10 Input Impedance:

Input impedance is defined as "the impedance presented by an antenna at its terminals or the ratio of the voltage to current at a pair of terminals or the ratio of the appropriate components of electric to magnetic fields at a point."
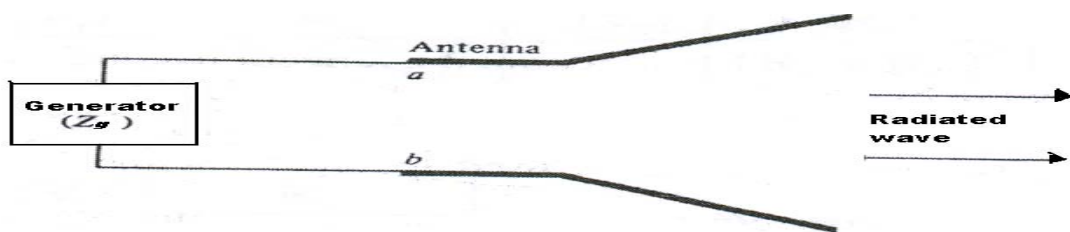
(a) Antenna in transmitting mode
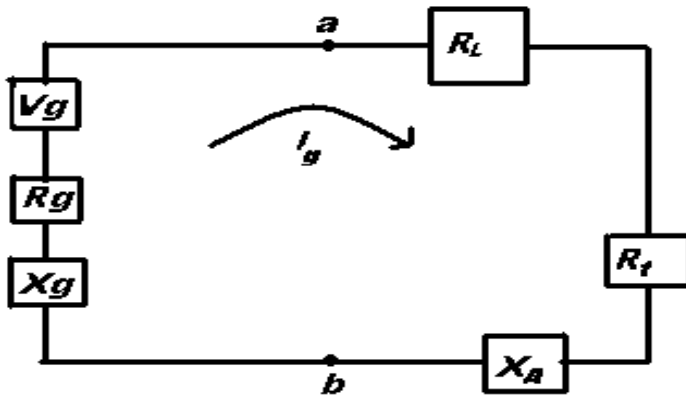
(b)Thevenin equivalent
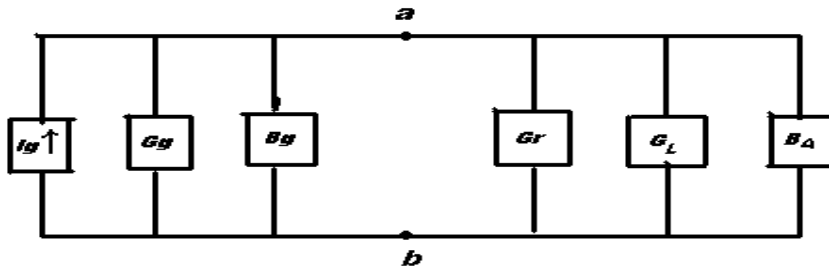
(c)Norton equivalent

Fig 6: Transmitting antenna and its equivalent circuit

Let us consider figure 6(a) where the terminals are designed as a-b . With no load attached the ratio of the voltage to current at these two terminals defines the impedance of the antenna as

$$Z_A = R_A + jX_A$$

Where

Z_A = antenna impedance at terminals a-b (ohms)

R_A = antenna resistance at terminals a-b (ohms)

X_A = antenna reactance at terminals a-b (ohms)

In general the resistive part of the Z_A consists of two components; that is

$$R_A = R_r + R_L$$

Where

R_r = radiation resistance of the antenna

R_L = loss resistance of the antenna

If we assume that the antenna is attached to a generator of internal impedance

$Z_g = R_g + jX_g$

where

Z_g = resistance of generator (ohms)

X_g = reactance of generator (ohms)

If the antenna is represented in transmitting mode we can represent the antenna and the generator by the equivalent circuit shown in figure 6(b). The current developed within the loop is given by

$$I_g = \frac{V_g}{Z_g} = \frac{V_g}{Z_g + Z_A} = \frac{V_g}{(R_r + R_L + R_g) + j(X_A + X_g)}$$

where V_g is the peak generator voltage.

And the magnitude is given by

$$|I_g| = \frac{|V_g|}{\left[(R_r + R_L + R_g)^2 + (X_A + X_g)^2\right]^{1/2}}$$

The power delivered to the antenna for radiation is given by

$$P_r = \frac{1}{2}|I_g|^2 R_r = \frac{|V_g|^2}{2}\left[\frac{R_r}{(R_r + R_L + R_g)^2 + (X_A + X_g)^2}\right]$$

and that dissipated as heat by

$$P_L = \frac{1}{2}|I_g|^2 R_L = \frac{|V_g|^2}{2}\left[\frac{R_L}{(R_r + R_L + R_g)^2 + (X_A + X_g)^2}\right]$$

The remaining power is dissipated as heat on the internal resistance of the generator and is given by

$$P_g = \frac{1}{2}|I_g|^2 R_g = \frac{|V_g|^2}{2}\left[\frac{R_g}{(R_r + R_L + R_g)^2 + (X_A + X_g)^2}\right]$$

The maximum power delivered to the antenna occurs when we have conjugated matching; that is when

$R_r + R_L = R$

$X_A = -X_g$

In that case

$$P_r = \frac{|V_g|^2}{2}\left[\frac{R_r}{4(R_r+R_L)^2}\right] = \frac{|V_g|^2}{8}\left[\frac{R_r}{(R_r+R_L)^2}\right]$$

$$P_L = \frac{|V_g|^2}{8}\left[\frac{R_L}{(R_r+R_L)^2}\right]$$

$$P_g = \frac{|V_g|^2}{8}\left[\frac{R_g}{(R_r+R_L)^2}\right] = \frac{|V_g|^2}{8}\left[\frac{1}{R_r+R_L}\right] = \frac{|V_g|^2}{8R_g}$$

From equation (2.11) and (2.13) it is evident that

$$P_g = P_r + P_L = \frac{|V_g|^2}{8}\left[\frac{R_g}{(R_r+R_L)^2}\right] = \frac{|V_g|^2}{8}\left[\frac{R_r+R_L}{(R_r+R_L)^2}\right]$$

The power supplied by the generator during conjugate matching is

$$P_S = \frac{1}{2}V_g I_g = \frac{1}{2}V_g\left[\frac{V_g}{2(R_r+R_L)}\right] = \frac{|V_g|^2}{4}\left[\frac{1}{R_r+R_L}\right]$$

The power that is provided by the generator, half is dissipated as heat in the internal resistance (R_g) of the generator and the other half is delivered to the antenna. This only happens when we have conjugate matching. Of the power delivered to the antenna one part is radiated by the antenna through the mechanism provided by the radiation resistance and the other part is dissipated as heat that is influential in the overall efficiency of the antenna. For a lossless antenna one half of the total power supplied by the generator is radiated by the antenna during conjugate matching and the other half is dissipated as heat in the generator. Thus to radiate half the available power through R_r the other must be dissipated as heat in the generator through R_g. In the receiving mode of the antenna these two powers are analogous to the power transferred to the load and the power scattered by the antenna. If there is a transmission line between the two, as usually the case, then Z_g represents the equivalent impedance of the generator transferred to the input terminals of the antenna. Figure 6(c) illustrates the Norton equivalent of the antenna in transmitting mode.
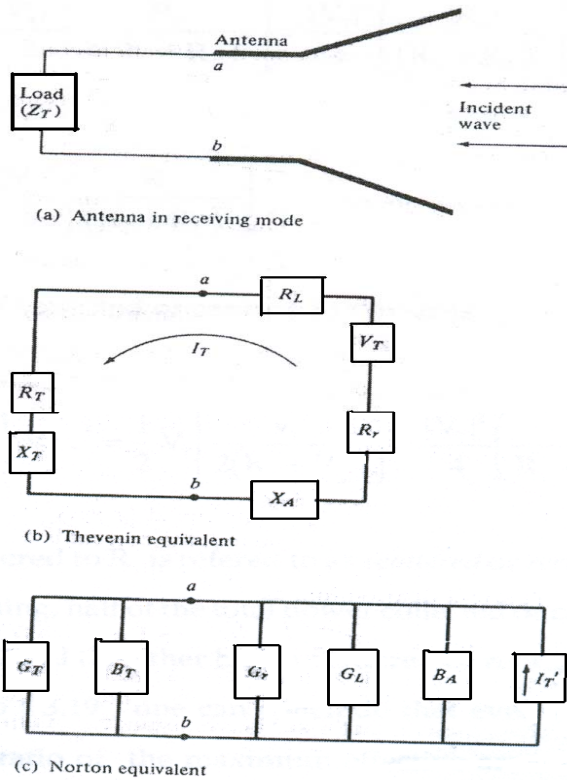
Fig 7 Antenna and its equivalent circuit in receiving mode

When the incident wave impinges upon the antenna it induces a voltage V_T which is analogous to V_g in the transmitting mode. The Thevenin's equivalent circuit of the antenna and its load (R_T) is shown in the figure 7(a) and the Norton equivalent circuit in receiving mode is shown in figure 7 (c). In the similar procedure it can be shown that for receiving mode under conjugate matching $(R_r + R_L = R_T$ and $X_A = -X_T)$ the power delivered to R_T, R_r and R_L are given as

$$P_T = \frac{|V_T|^2}{8}\left[\frac{R_T}{(R_r+R_L)^2}\right] = \frac{|V_T|^2}{8}\left[\frac{1}{R_r+R_L}\right] = \frac{|V_T|^2}{8R_T}$$

$$P_r = \frac{|V_T|^2}{2}\left[\frac{R_r}{4(R_r+R_L)^2}\right] = \frac{|V_T|^2}{8}\left[\frac{R_r}{(R_r+R_L)^2}\right]$$

$$P_L = \frac{|V_T|^2}{8}\left[\frac{R_L}{(R_r+R_L)^2}\right]$$

While the induced (collected or captured) power is

$$P_C = \frac{1}{2}V_T I_T{}^* = \frac{1}{2}V_T\left[\frac{V_T^*}{2(R_e+R_L)}\right] = \frac{|V_T|^2}{4}\left[\frac{1}{R_r+R_L}\right]$$

The power P_r delivered to R_r is referred to as scattered or reradiated power. Thus under the conjugate matching, half of the total power collected or captured is delivered to the load R_T and the other half is scattered or radiated through R_r. Using the value of P_T to P_C one can conclude that even though the aperture efficiencies, which is the ratio of the maximum effective area to physical area, are higher than 50%, all of the power that is captured by the antenna is not delivered to the load but it includes that, which is scattered plus dissipates as heat, by the antenna. The most that can be delivered to the load is only half of that captured and then will be only under conjugating matching and lossless transmission line.

2.1. Introduction:

GMRT stands for Giant Meter-wave Radio Telescope. Mainly a radio telescope in its simplest form consist of three components (i) an antenna that selectively receives radiation from a small region of the sky,(ii) a receiver that amplifies a restricted frequency band from the output of the antenna and (iii) a recorder for registering the receiver output. The GMRT antennas are mainly the parabolic reflector antennas. From the invention of the parabolic antenna by Sir Heinrich Hertz in 1888 to demonstrate the existence of the electromagnetic waves to the construction of the reflector antenna by Sir Marconi for the investigation of the microwave propagation leads to a tremendous progress in the history of antenna designs. Later in 1937, Sir Grote Reber constructed the prototype of modern dish antenna, was a prime focus parabolic reflector antenna of 9.1m diameter, which he used to make the first radio maps of the sky.

2.2. Antennas Types for Radio Astronomy:

From the helical antennas to the parabolic antenna diverse variety of antennas have been used for radio astronomy, the principal reason behind this is to have a wide range of observing wavelengths. The most common antenna used for radio astronomy is the parabolic reflector with either prime focus feeds or cassegrain type feed arrangement. Prime–focus parabolic antenna although mechanically simple has certain disadvantages such as (i) the image forming quality is poor due to lower f/D ratios, and (ii) the feed antenna pattern extend beyond the edge of the parabolic reflector and hence picks up some thermal radiation from the ground. Cassegrain antenna is a double reflector system which works on the principle of cassegrain optical telescope. It employs a parabolic contour for the main dish and a hyperbolic contour for the sub dish. One of the two foci of the hyperbola is the real focal points of the system and is located at the center of the feed; the other is a virtual focal point which is located at the focus of the parabola. Cassegrain antenna permits a reduction in the axial dimensions of the antenna just as in optics and also permits greater flexibility in the design of the feed system.
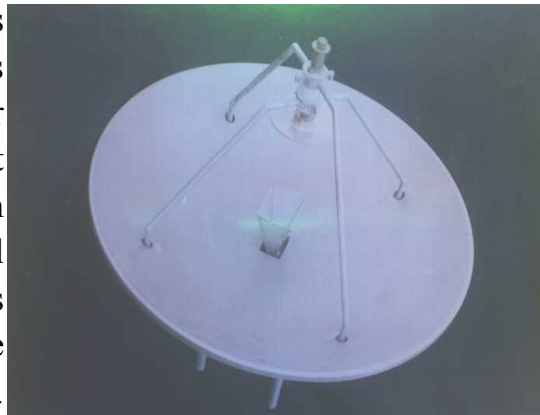
Cassegrain geometry allows placement of the RF plumbing behind the reflector which eliminates the need for long transmission lines. A high gain cassegrain reflector antenna in Ku-band has been successfully developed for command transmits application for the missile programme. It can also be used for mono pulse radar, satellite communication, etc.

But in GMRT the antennas are based on Prime-focus system. The primary advantages of the parabolic antennas are the ease with which receivers can be coupled to it. The input terminals are at the feed horn or dipole. It gives a high gain ($\approx$ 25dB for aperture diameters as small as 10λ is easily available), also full steer-ability, general either by polar or azimuth-elevation mounting. Further the antenna characteristics are to first order independent of pointing. It can handle a wide range of operating wavelength simply by changing the fed and focus. Generally for radio astronomy parabolic reflectors are having short f/D ratio as compared to optical reflectors. Highly curved reflectors required for higher f/D ratios result in increased cost and reduced collecting areas. The reflecting antennas re to first order frequency independent, there is nonetheless a finite range of frequencies over which a given reflector can operate. The shortest operating wavelength is determined by the surface smoothness of the parabolic reflector. If λ_{min} is the shortest wavelength then,

$$\lambda_{min} \approx \sigma/20 \quad \text{.. (i)}$$

where, σ is the rms deviation of the reflector surface from a perfect paraboloid. Below λ_{min} the antenna performance degrades rapidly with decrease wavelength. The longest wavelength is governed by diffraction effects. As given rule of thumb the largest operating wavelength λ_{max} is given by

$$\lambda_{max} < 2L \quad \text{.. (ii)}$$

where L is the mean spacing between the feed support legs. At $\lambda = L$ the feed support structure would completely shadow the reflector.

2.3. Specification of the GMRT Antennas:

GMRT antennas are having a f/D ratio fixed at the value 0.412 based both on structural design issues as well as depending on various feed radiation patterns. Since the antennas mainly works at meter wavelength prime focus feeds were preferred. Cassegrain feeds at meter wavelengths would results in

impractically large and concomitant large aperture block-age. Six bands of frequencies had been identified for GMRT operation. As it is essential to be able to change the observing frequency rapidly, consequently the feeds had to mount on a rotating turret placed at the prime focus.

Fig shows one of the GMRT antennas

The feeds are mounted on the orthogonal faces of a rotating faces. Since one needs six frequency bands, this leads to the constraint that at least two faces of the turret should support dual frequency capability. For astronomical reason also dual frequency capability was highly desirable.

The reflector surface of the GMRT antennas is not perfectly reflective and hence the transmission losses through the mesh have to be taken into account. Further the expected surface errors of the mesh panels were   5mm. This implies that the maximum usable independent of the loss seems to be 3000 MHz, since the mean spacing of feed support legs, L = 23.6m, the lowest usable frequency is around 6MHz.

2.4. Feeds used at GMRT:

2.4.1. Feeds Placement:

 As mentioned above the feeds are placed in orthogonal faces of a rotating cube. The phase centres of the entire cube are coincident with the paraboloid focus. The space between the turret and the feed is utilized for mounting the front-end electronics; there are six bands altogether, 1000-1450 MHz, 610 MHz, 327 MHz, 233 MHz, 150 MHz and 50 MHz. The 50 MHz feed is fixed to the support legs and not on to the turret. As such it is in focus at all the times. The 610 MHz and 233 MHz feeds are mounted on the same turret face.
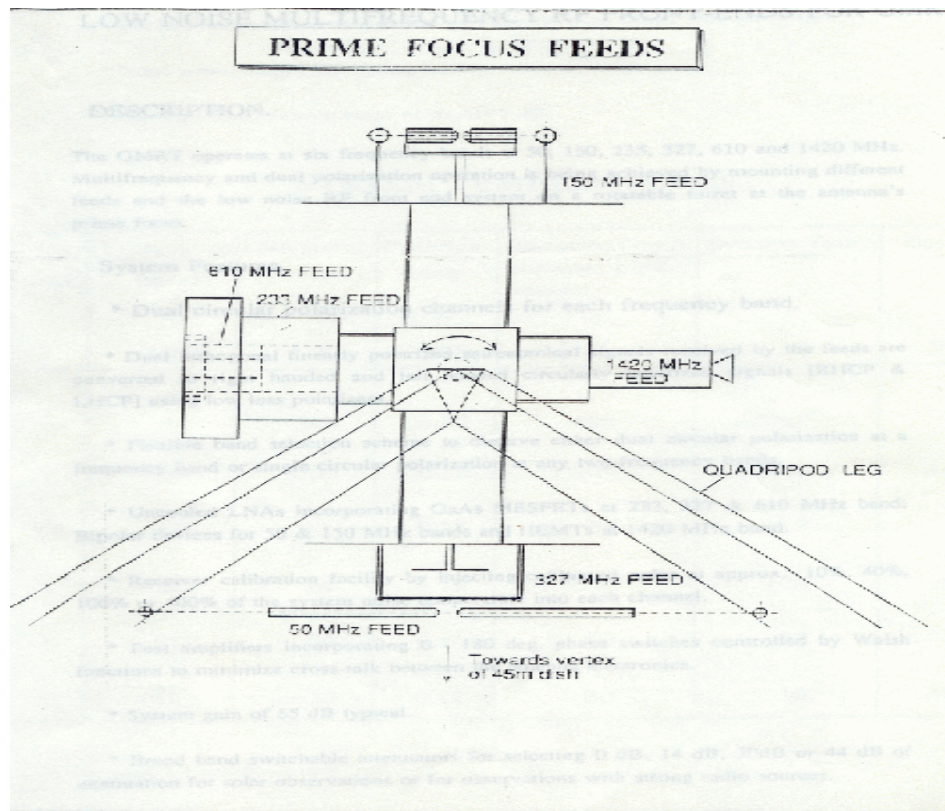
Fig shows the feeds mounted in the turret

2.4.2. 150 MHz Feed:

 This feed consists of four dipoles in a boxing ring configuration, placed above a plane reflector. The dipole is a wide band one i.e. has an octave bandwidth. It is a folded with each arm being a thick dipole (diameter $d >0.05$),

sinusoidal current distribution can be assumed for the computation of input impedance and related radiation pattern for such dipoles. Crossed-dipoles are used to give sensitivity to both polarizations. For this design the cross dipole configuration is somewhat complex hence a boxing ring configuration was given. Here one pair of dipoles at $\lambda/2$ spacing provides sensitivity to one linear polarization. Another pair orthogonally oriented with respect to the first pair gives sensitivity to the orthogonal polarization. Feed dimensions are given below:

- Folded dipole length: 0.39λ
- Dipole height above reflector: 0.29λ
- Reflector (diagonal of octagon) : 1.2λ

The dipoles have an *l/d* ratio of 6.48, and the phase center was determined to be at a height of 100mm above the reflector.

2.4.3. 327 MHz Feed:

A dipole has a broader H pattern than its E pattern, but it is necessary to have a matched E and H plane for achieving a good cross polarization properties. This pattern is achieved by placing a conducting ring above the dipole, parallel to the reflector and is supported by dielectric rods. This is called as the beam forming ring or simply BFR introduced by P.S. Kildal. The beam forming ring compresses the H plane while it has no significant effect on the E plane. The measurement value of the prototype 327 MHz model is given below:

- Reflector diameter: 2.2λ
- Height of the dipole above the reflector: 0.26λ
- BFR diameter: 1.22λ
- BFR height above the reflector: 0.51λ

The measured phase centre is at 26mm above the reflector for both E and H planes. Crossed dipoles are employed for dual polarization. Sleeves are introduced over the dipoles to increase the bandwidth of the feed, this design deviates the feed from actual Kildal design. The linear polarized outputs of the dipoles are mixed in a quaqdrature hybrid at one end of the front end chassis to produced two circular polarized signals, which go further into the amplifying, signal conditioning circuits of front-end electronics.

2.4.4. Dual-Frequency Coaxial Waveguide Feed:

The 610 MHz and 233 MHz feeds are dual frequency coaxial feeds. The single most attractive features of the coaxial waveguide feed is its multi-frequency launching capability. Simultaneous transmission or reception of well separated frequencies is possible. This type of feed of has been used as on board satellite antennas to provide coverage at three frequency bands.

The design of the GMRT 610 MHz/233 MHz waveguide feeds is based on an exhaustive theoretical analysis of the design of coaxial waveguide feeds. A constraint in such multi frequency designs is that adjacent frequency bands should not overlap to within an octave. The 150 MHz could have been combined but it would result in unwieldy dimensions of the feed. The fundamental mode of propagation in coaxial structures is TEM; hence the radiated field component along the axis is zero everywhere. So propagation by an alternate mode (single or multimode) is essential to get rid of the undesired characteristics. Coaxial waveguides must then be forced to radiate in TE_{11} mode. This is achieved simply by exciting the probes in phase opposition (low loss baluns are essential in such design).

In dual frequency construction the outer conductor of the 610 MHz serves as the inner one for the 233 MHz . Quarter wavelength chokes are provided in both the frequency parts to cut down the surface currents on the outer conductor and thereby ensure pattern symmetry. The waveguide feeds have two pairs of probes. One pair supports a given planner polarization while orthogonal pair supports the orthogonal polarization. Similar to the dipole feed, a quaqdrature feed hybrid at the back end of the coaxial feed is used to convert the linear polarization to circular polarization. The rear-half of the 610 MHz feed, separated by a partition disc, is utilized to accommodate the baluns, quadrature hybrid, LNA's of 610 MHz and 233 MHz The overall dimensions of the feed are given below:

- Aperture diameter: 0.9λ (- 610 MHz) 0.85λ (- 233 MHz)
- Wavelength cavity length: 0.95λ (-610 MHz) 0.73λ (- 233 MHz)

The phase center is not at the aperture plane, but at a point 60 mm in front of the aperture. As needed the radiation pattern of the one coaxial feed does not shows any significant change due to the presence of the other coaxial waveguide part.

2.4.5. 1000 – 1450 MHz Feed:

This feed is a corrugated horn type, known for its high aperture efficiency and very low cross polarization levels. In any horn, the antenna pattern is severely affected by the diffraction from the edges which can lead to undesirable radiation not only in the back lobe but also in the main lobe. By making grooves on the horn on the walls of a horn, the spurious diffraction is eliminated. Such horns are called "corrugated horn". This feed at 1420 MHz has fins instead of grooves since whole assembly is made out of brass metal sheet. The flare-angle of the horn is 120°. The dimensions of the feed are given as follows:

- Aperture diameter: 3.65λ
- Horn length: 4.48λ

The phase center has been found out to be at the apex of the cone – at a depth of 200 mm from the aperture plane. The bandwidth of this feed is found out to be 580MHz, starting from 1000 MHz to 1580 MHz The entire band is divided into four sub-bands each 140 MHz wide and cantered on 1390, 1280, 1170 and 1060 MHz . There is also a bypass mode in which the entire band width is available.

Fig shows the feeds mounted on the turret (GMRT)

3.1. WIPL-D Introduction:

It is basically a 3D electromagnetic solver program which allows fast and accurate analysis of metallic, dielectric, magnetic structures (antenna, scatterers, passive microwave circuit etc.). The calculations are done in frequency domain. It is an user friendly program enables you to define the geometry of any structure in any interactive way as a combination of wires, plates and material objects. As an output WIPL-D provides the current distribution on the structure, radiation pattern, near field distribution, admittance, and S-parameters at the predefined feed points. It also provides a variety of printer based and graphics output capabilities, including 2D and 3D graphs of the parameters of interest.

Key Features:
- The composite structure is characterized by equivalent surface electric currents over metallic portions and equivalent surface electric and magnetic currents over dielectric material surfaces. In this code it is possible to include loss materials with complex permeability and permittivity.
- Concentrated and distributed loadings may be applied to the metallic structure, thus stimulating lumped elements, losses due to the skin effect, surface roughness etc.
- Flexible geometrical modelling includes cylindrical and conical wires, quadrilateral plates which may characterize metallic or lossy/lossless dielectric/magnetic surfaces, wire to plate junction, and protrusions, so that almost any finite composite structure can be precisely modelled.
- Accurate current modelling is based on polynomial approximation in conjunction with Galerkin method applied to surface integral equations, resulting in an accurate and efficient method.
- Custom codes include generation of complex objects (like BOR, BOT, etc.) manipulation with WIPL-D entities (rotating, scaling, multiplication, etc.) importing of all ready defined structures, and symbolic dimensioning of the structures, providing an environment of fast creation of new and easy modification of old structures.
- A variety of graphic plotting options are available, like overlaying 2D graphs from different projects, or colouring and shading 3D drawings of edited structure.

3.2. Basics of Antenna Design:

Basically the antenna design mentioned is refer to the electromagnetic modelling of metallic structures. In the electromagnetic modelling the main goal of the analysis is to determine the surface current distribution over the structure which results due to the induced charges and current because of the incident of the time harmonic electromagnetic field (E & H) of angular frequency ω on it. This goal can be achieved in two principal steps:

- The first step is the description of the structure geometry. It can be or defined exactly or approximately.
- The second step is the determination of the currents over the (exact or approximate) geometrical model for a given incident (impressed) field distribution.

Now reference to the above the analysis of the problems of the electromagnetic modelling can be divided into three parts:

1. Geometrical modelling
2. Modelling of currents
3. Evaluation of antenna and scattered characteristics

3.2.1. Geometrical modelling:

An arbitrary metallic structure can be considered to be composed of appropriately interconnected plates and wires. From the view point of electromagnetic modelling, the plate is infinitesimally thin and made up of a perfect conductor. There is no field inside the closed plate structure. In a 3D plane the plate can be placed by forming four nodes each node defining by the (x, y, and z) co-ordinates. Moreover a wire and its length is defined by two nodes in the 3D plane, the radius can be given on the wire placing window that appears on the screen. The junction of plates is modelled with plates having two common edges. The junction of wires is modelled by wires that have common nodes. As mentioned wires can be modelled by plates. In this case, the geometry of a wire plate junction is modelled in the same way as the geometry of a plate to plate junction. Thus geometrical modelling of the desired structure can be made. More details of the modelling will be discussed later.

3.2.2. *Modelling of currents:*

Modelling of currents is based on the solution of the electric field integral equation. The current is approximated by a finite sum of known functions multiplied by unknown coefficients. These coefficients are obtained by applying the method of moments to EFIE.

Electric Field Integral Equations:

Let us consider a perfect conducting structure situated in a vacuum and excited by an incident electric field E_i. In that case, the boundary conditions require that the tangential component of the total electric field be zero on the structure surface that is

$$(E + E_i)_{tang} = 0 \qquad ....(i)$$

where E is the electric field produced by the currents and charges induced over the structure surface.

For obtaining the value of EFIE in case of plates we are to placed the value of E in (i) as

$$E = -j\omega\mu_o\left\{\int_S J_s g(R)dS + \frac{1}{\beta^2}\int_S div_s J_s \, i_R \frac{dg(R)}{dR}dS\right\} .... \text{(ii)}$$

Where

J_s is the surface current density

$g(R) = \dfrac{e^{-j\beta R}}{4\pi R}$; $\beta = \omega\sqrt{(\mu_o\varepsilon_o)}$ is the phase coefficient

R is the distance between the field point and the source point

i_R is the unit vector directed from the source point to the field point

For obtaining the value of EFIE in case of wire we put the value of E in (i) as

$$E = -j\omega\mu_o\left\{\cos\alpha i_z \int_{S_1}^{S_2} I(s)g(R_e)\,dS + \frac{1}{\beta^2}\int_{S_1}^{S_2} \frac{dI(s)}{ds} grad(R_e)\frac{dg(R_e)}{R_e}ds\right\}...... \text{(iii)}$$

Where

$I_s =$ the total current flowing through the wire or the truncated cone

R_e is the distance between field point and the source point

α is the angle between the cone axis and the cone geometrics

Treatment of Excitation:

Scatterers are excited by plane waves. Let's assume that the wave is incident on the structure from the direction defined by the unit vector 'n$_i$'. Let the wave be elliptically polarized and the co-ordinate origin as the phase reference point. The expression for the (complex) electric field of the wave is then of the form

$$E_i(r) = E_{io} e^{-j\beta r.n_i} \quad \dots\dots\dots\dots\dots\dots\dots\dots\dots\dots\dots\dots\dots\dots \text{(iv)}$$

the unit vector n is completely determined by the θ and Φ- angles of arriving direction. The complex electric vector in the co-ordinate origin is completely determined by its θ and Φ- components.
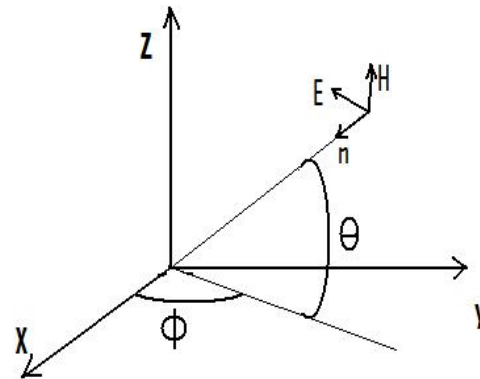
Antennas are excited by voltage generators. Two types of generators are considered:

- Delta-function generator: it is a point like ideal voltage generator. This generator is defined in several ways. The simplest way is to require that the potential difference between two infinitely small close points of generator terminals is equal to the desired EMF of the generator. Theoretically, this generator can't be used for excitation of cylindrical wires since the capacitive currents between two driven dipole bases are infinitely large. Low- order approximation of current along the dipole can't follow this rise in current intensity in the immediate vicinity of the excitation if the dipole is not relatively fat.

- Co-axial line excitation: they are mainly used in the excitation of the monopole antennas that lies above the finite ground.

The Galerkin Method:

The EFIE belongs to the class of linear operator equations. It can be written in the form

$$Lf(\mathbf{r}) = g(\mathbf{r'}) \quad \dots\dots\dots\dots\dots\dots\dots\dots\dots\dots\dots\dots\dots\dots \text{(v)}$$

where L is the known linear operator, g(r') is a known function, and f(r) is a unknown function that should be determined. **r** is a vector position of the source points , and **r'** is a vector position of the field point distributed over the surface of the plates and along the axis of the wires. The equation (v) actually represents an infinite number of linear algebraic equations for an infinite number of unknown values of current over plates and along wires. It can be solved by the method of moments in the following way. The unknown function **f** is approximated by an infinite sum in the form

$$f(\boldsymbol{r}) = \sum_{i=1}^{N} a_i f_i(\boldsymbol{r})$$ .... (vi)

where N is the order of approximation, a_i , i = 1, 2, 3, ..., N, are known coefficient to be determined and $f_i(\boldsymbol{r})$, i = 1,..,N, are known basis functions. Substituting this expansion into (v), the linear operator equation is written in the form

$$\sum_{i=1}^{N} a_i Lf_i(\boldsymbol{r}) = g(r')$$ .... (vii)

Since the number of unknowns in the upper equation is limited to N, this equation can only be approximately satisfied over the plates and along the wires. In order to determine these unknowns, the above equation should e transformed into the system of N linear algebraic equations. This system of equations can be obtained if N independent operations are performed over the left and right side of the above equation, in such a manner that variable **r'** is eliminated. Multiplying $f_j(\boldsymbol{r'})$ on both side of equation (vii) and integrating over the plate or wire for which $f_j(\boldsymbol{r'})$ is defined, the following linear algebraic equation of the form is obtained

$$\sum_{i=1}^{N} a_i \int_{S_i} f_j(r') Lf_i(r) dS_j = \int_{S_j} f_j(r') g(r') dS_j$$ .... (viii)

where j = 1,............, N

A similar set of equations can be written in the case of composite wire and plate structure. The functions that are used for multiplication of the left and right side of (vii) are known as the test functions. Hence, this last stage of the method of moments is known as the test procedure. If the test function is equal to the basis function, as in this work, the test procedure is referred to as a Galerkin test procedure. The resulting system of linear equation is solved by using the L-U decomposition which gives the coefficients of the current expansion.

3.2.3. Evaluation of Antenna and Scatterer Characteristics:

Once the unknown coefficients of current expansion are determined, the required electrical properties of the structure analyzed can be computed with relative ease. In this work, the following characteristics are evaluated:

- Network parameters,
- Current distribution,
- Far field,
- Near field

An antenna is a structure with at least one port, excited at its ports by at least one ideal voltage generator. With respect to the generators, the antenna behaves like a passive network. Generally, for an antenna with N ports, the complex port currents and the complex port voltages are related by linear algebraic equations in the form

$$I_1 = y_{11}V_1 + y_{12}V_2 + \ldots + y_{1N}V_N$$

$$I_2 = y_{21}V_1 + y_{22}V_2 + \ldots + y_{2N}V_N \quad \ldots\ldots\ldots\ldots\ldots\ldots\ldots\ldots\ldots\ldots \quad \text{(ix)}$$

$$\ldots\ldots\ldots\ldots\ldots\ldots\ldots\ldots\ldots\ldots\ldots\ldots$$

$$I_N = y_{N1}V_1 + y_{N2}V_2 + \ldots + y_{NN}V_N$$

where y_{ij}, $i,j = 1,\ldots\ldots, N$, are complex coefficients called the admittance (y) parameters of the network. The set of above equations is usually put into matrix form

$$[I] = [y][V] \quad \ldots\ldots\ldots\ldots\ldots\ldots\ldots\ldots\ldots\ldots\ldots\ldots\ldots\ldots\ldots\ldots\ldots\ldots\ldots\ldots\ldots \text{(x)}$$

Where [I] is a column matrix containing the port current, [V] is a column matrix containing the port voltages, and [y] is a square matrix of the impedance parameters.

Similarly the complex port voltages are express as a linear combination of the complex port currents, which is written in the matrix form as

$$[V] = [z][I] \quad \ldots\ldots\ldots\ldots\ldots\ldots\ldots\ldots\ldots\ldots\ldots\ldots\ldots\ldots\ldots\ldots\ldots\ldots\ldots\ldots \text{(xi)}$$

Instead of the port voltages and currents, at high frequencies, intensities of two waves travelling at the transmission lines connected to the ports are often considered. The intensities of the waves travelling to and from the network

("incident wave" and "reflected wave") at the ith port are defined as

$$a_i = \frac{V_i + Z_{ci}\, I_i}{2\sqrt{Z_{ci}}} \quad ; \quad b_i = \frac{V_i - Z_{ci} I_i}{2\sqrt{Z_{ci}}} \quad \dots\dots\dots\dots\dots\dots\dots \text{(xii)}$$

where Z_{ci} is the nominal impedance of the ith port. These coefficients can also be related in the matrix form as

$$[b] = [s][a]$$

Where $[s] = \begin{bmatrix} S_{11} & S_{1N} \\ & \ddots & \\ S_{N1} & S_{NN} \end{bmatrix}$ .... (xiii)

here S_{ij}, $i,j = 1,..., N$ are complex coefficients called the scattering (s) parameters of the network. Most often in practice, the nominal impedances are 50Ω. Nominal impedances used by WIPL-D are always 50Ω.

For the far if the from the field point to the antenna is much greater than the maximal dimension of the antenna is much greater than the wavelength, the electric vector is written in the form

$$E(r, \Phi, \theta) = e(\Phi, \theta)\frac{e^{-j\beta r}}{r} \quad \dots\dots\dots\dots\dots\dots\dots \text{(xiv)}$$

where r, Φ, θ are spherical coordinates and β is the free-space phase coefficient. The vector e (Φ, θ) will be referred to as normalized electric field. It should be noted that the electric field vector has only Φ and θ components. The corresponding magnetic field is expressed as

$$H(r, \Phi, \theta) = \frac{1}{Z_o} i_r \times E(r, \Phi, \theta) = \frac{1}{Z_o}[i_r \times e(\Phi, \theta)]\frac{e^{-jkr}}{r}$$

$$Z_o = \sqrt{\frac{\mu_o}{\varepsilon_o}} \quad \dots\dots\dots\dots\dots\dots\dots\dots \text{(xv)}$$

where Z_o is the wave impedance of the vacuum and i_r is the unit vector in the radial direction. The corresponding Poynting vector is given by

$$P(r, \Phi, \theta) = E(r, \Phi, \theta)\, H^*(r, \Phi, \theta) = \frac{|E(r,\Phi,\theta)|^2}{Z_o} i_r = \frac{|e(\Phi,\theta)|^2}{Z_o r^2} \quad \dots\dots\dots \text{(xvi)}$$

From the above equations, we see that the electric vector, the magnetic field vector, and the Poynting vector can be easily evaluated at any far field point if the normalized electric field is known.

3.3 Working with the Software:

After getting introduced with the software it is easier to know how it works. For defining an antenna the geometrical modelling of the antenna is a must in the 3-D plane. The following are the entities that determine the antenna model or simply we can say the metallic structure: "nodes", "wires", "plates", and "junctions". All metallic structures are grouped into three classes:

- Wire structures
- Plate structures
- Combined wire and plate structures

Variables can be defined for defining certain measuring values such as defining certain distance of a node from origin or radius of a wire etc.

Wire Structures:

In general, WIPL-D can handle wire structures consisting of arbitrary wires interconnected in an arbitrary way and situated in free space. Wires can be placed in the 3-D plane in a position desired by defining the nodes in the plane as shown below. The radius of the wire can be defined easily by the user in the window open for placing the wire between the nodes.
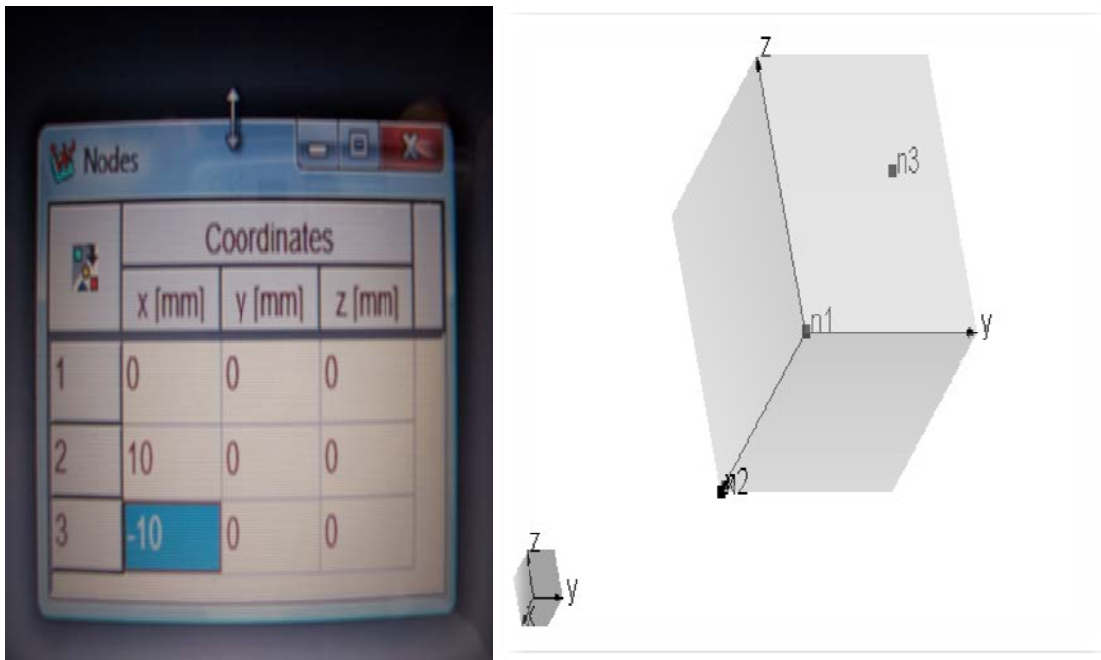
Fig: shows defining of nodes and there placement in the 3-D plane
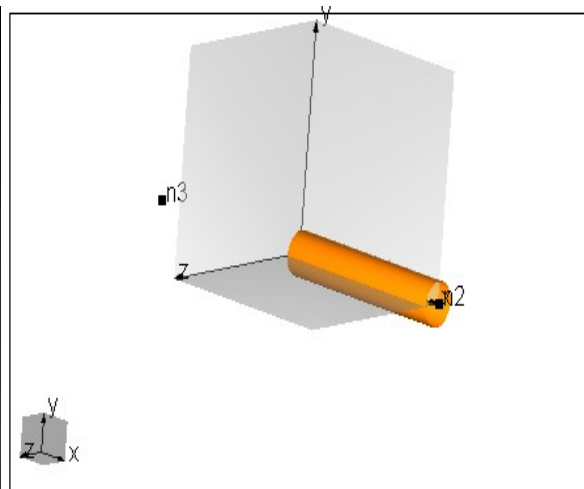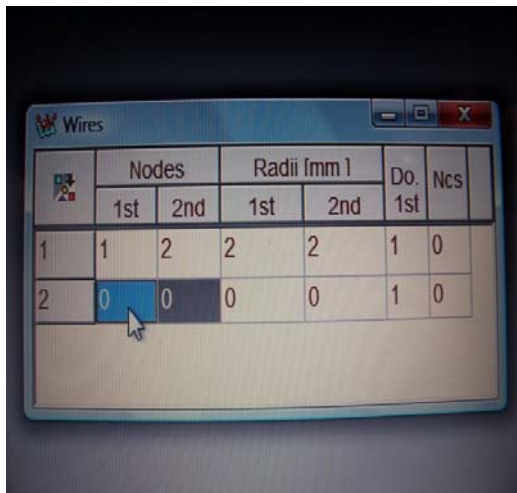
Fig: shows defining a wire placed in between the nodes defined earlier.

In this section only straight wires are considered, curved wires can be modelled by a sequence of straight wires. There is no difference between solid and hollow wires if they are thin enough. The thick hollow wires are more precisely modelled as pipes made up of plates. All wire to wire junctions are presented as junctions of wire ends.

Plate Structures:

WIPL-D can handle plate structure consisting of arbitrary plates interconnected in an arbitrary way and is situated in free space. The plate is infinitesimally thin and made up of a perfect conductor. There is field inside a closed structure composed of plates. A plate is placed in the 3-D plane in between four nodes as defined by the user as shown below. It is obvious that in a particular case, the basic plate element has the form of a flat quadrilateral, rectangle, square and so on. (Fig. shows defining of plates with the nodes)
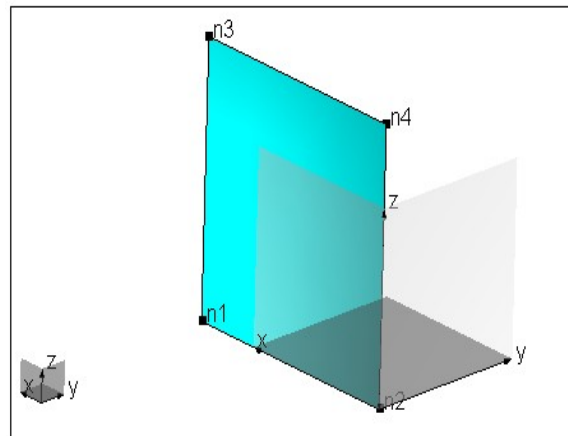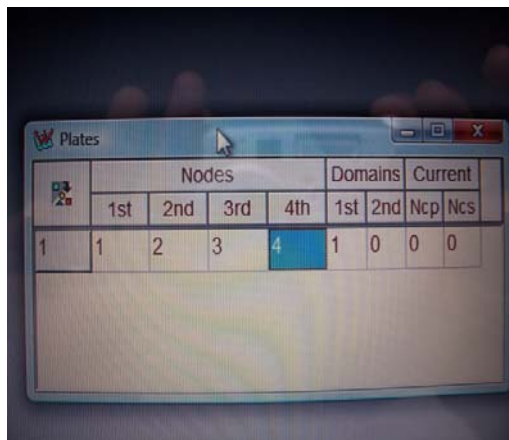
All plate-to-plate junctions are presented as junctions of plate edges. There are twobasic classes of such plate-to-plate junctions:

- All plates at a junction have two common nodes, defining a common edge.
- Electrically short edges of all plates don't coincide and are situated in an electrically small junction domain.

Composite Wire and Plate Sructures:

In general, any metallic structure can be modeled as a composite wire and plate structure. All composite wire and plate structures can be grouped into two main classes:

- Structures without wire-to-plate junctions
- Structures with wire-to-plate junctions

A simple wire-to-plate structure without a wire-to-plate junction represents a simple combinationof a wire structure and a plate structure. In case of composite wire and plate structures with wire-to-plate junctions, can be grouped into two classes:

- Simple wire-to-plate junction
- Combined wire-to-plate junctions

The simple wire to plate junction contians one wire end and one short plate edge situated in an electrically small domain. Any other wire to plate junction can be represented as a combination of simple wire to plate junctions. Hence, they are referred to as combined wire to plate junctions.

OBJECTS:

These are compound WIPL-D entities made up of wires and plates that belonging to different domain. Various objects made up of plates can easily be created by the object edition. We can say that there are some inbuilt structures that can be varied by varying the variable parameters. ThE Odjects descriptor creates and modifies the highlighted object in the Objects list. The Objects descriptor consists of two Domains edit fields, seven Objects pages, and OK and cancel buttons. Two Domains edit firlds define order umbers of domains to which the object belongs.The active object pages describes the shape, size and

position of the object. In case of BoR, BoT, BoCC and BoCG geometrical models are created by the specifying generatrices.

Circles:

The circle object represents the geometrical model of a generalized circle or frill, as a whole or as a part, which can be extendedto a symetrical paraboloidal reflector. Inner and outer bounds of a generalized frill are super-quadric functions defined by the equation:

$$\left(\frac{x}{a_i}\right)^{\frac{2}{t_i}} + \left(\frac{y}{b_i}\right)^{\frac{t}{b_i}} = 1 \qquad i = 1,2...$$

where i = 1 stands for the inner bound, i = 2 for the outer bound. $2a_i$ and $2b_i$ represents the lengths of the axis along x and y coordinates and t is the Shape factor.
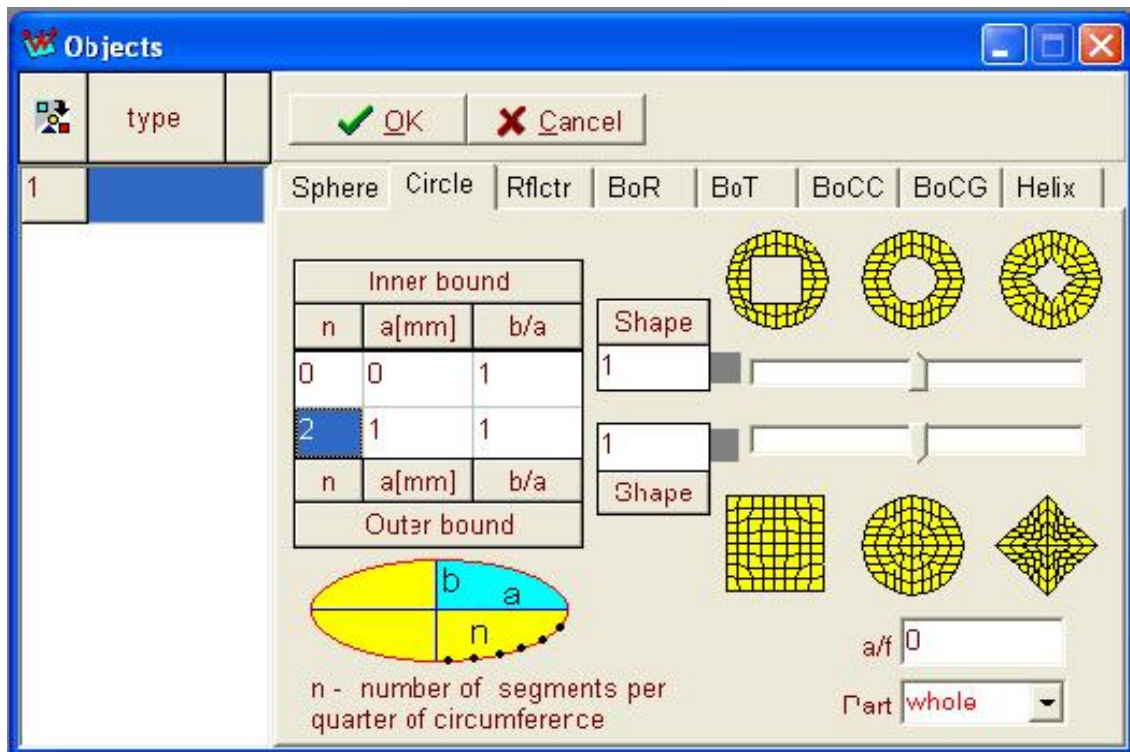
Fig. shows the object editor for placing circles

When the inner bound is omitted, generalized frill degenerates into generalized circle. When t is changed from 1 to 0 the object is transformed from circle to square. The shape and size of the original generalized circle are given by the parameters: a, b/a, a/f, and the Shape factor. In addition **n-** defines the number of segments per quarter of the circumference, **Part factor** defines at which part of the generalized circle should be created (whole, half, quarter, 1/8).

Sphere:

      The sphere object represents the geometrical model of a generalized sphere, in particular : sphere, ellipsoid, cube, box, octahedron, star etc. A generalized sphere is defined by the 3-D super quadratic equation:

$$\left(\frac{x}{a}\right)^{\frac{2}{t}} + \left(\frac{y}{b}\right)^{\frac{2}{t}} + \left(\frac{z}{c}\right)^{\frac{2}{t}} = 1$$

where a, b and c are the semi axes along the x, y and z-coordinates, and t is the Shape factor. When t is change from 1 to 0, the object is transformed from a sphere to a cube. When t is change from 1 to 2, the object is transformed from a sphere to an octahedron.
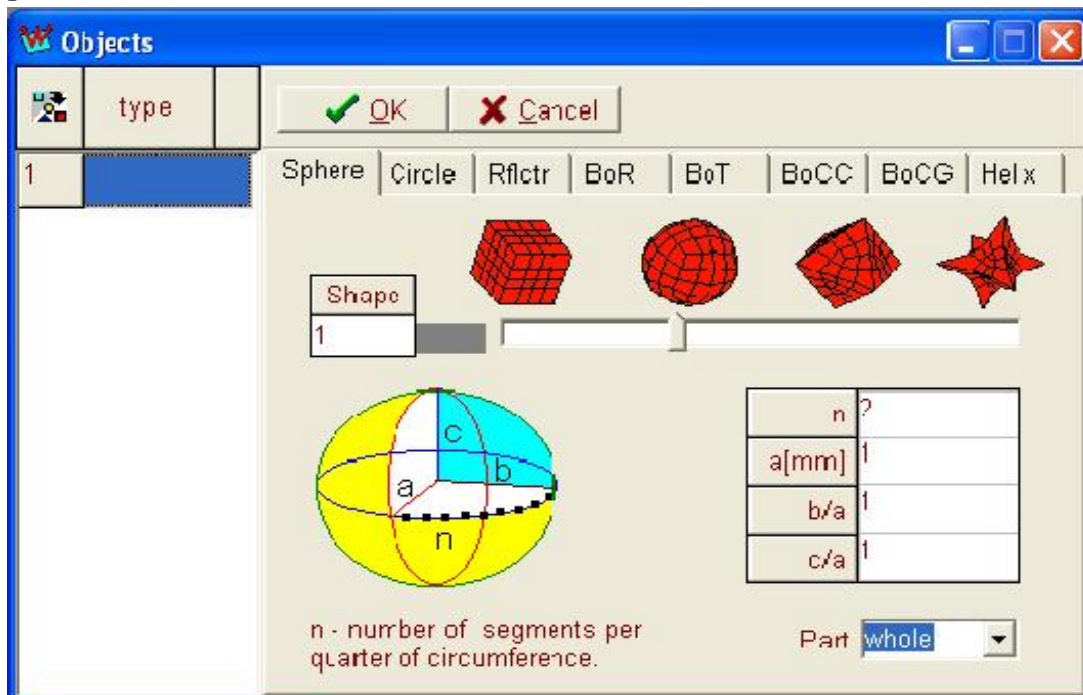
Fig. shows the object editor for placing sphere

The shape and size of an original generalized sphere are given by the parameters: a, b/a, c/a and t. In addition, choose: **n** – number of segments per quarter of circumference, **Part factor** – which part of the generalized sphere should be created (whole, half, quarter, 1/8).

BoR (Body of Revolution):

      The BoR represents the geometrical model of the body of revolution. The BoR is obtained when a piecewise linear generatrix, placed in the ρ-z plane, is rotated n times about the z- axis from φ_1 and φ_2 as shown in the window below. Generally, at the *i*th step during rotation, the body ρ- coordinates, ρ_{ij}, are scaled along the x-y generatrix as:

$$\rho_{ij} = \rho_{1i} \frac{x_{2i}i_x + y_{2j}i_y}{\sqrt{x_{21}{}^2 + y_{21}{}^2}}$$

where ρ_{1i} and z_{1i}, $i = 1...n_1$, are the coordinates of the ρ-z generatrix, and x_{1j} and y_{1j}, $j = 1,.....,n+1$, are the coordinates of the x-y generatrix.
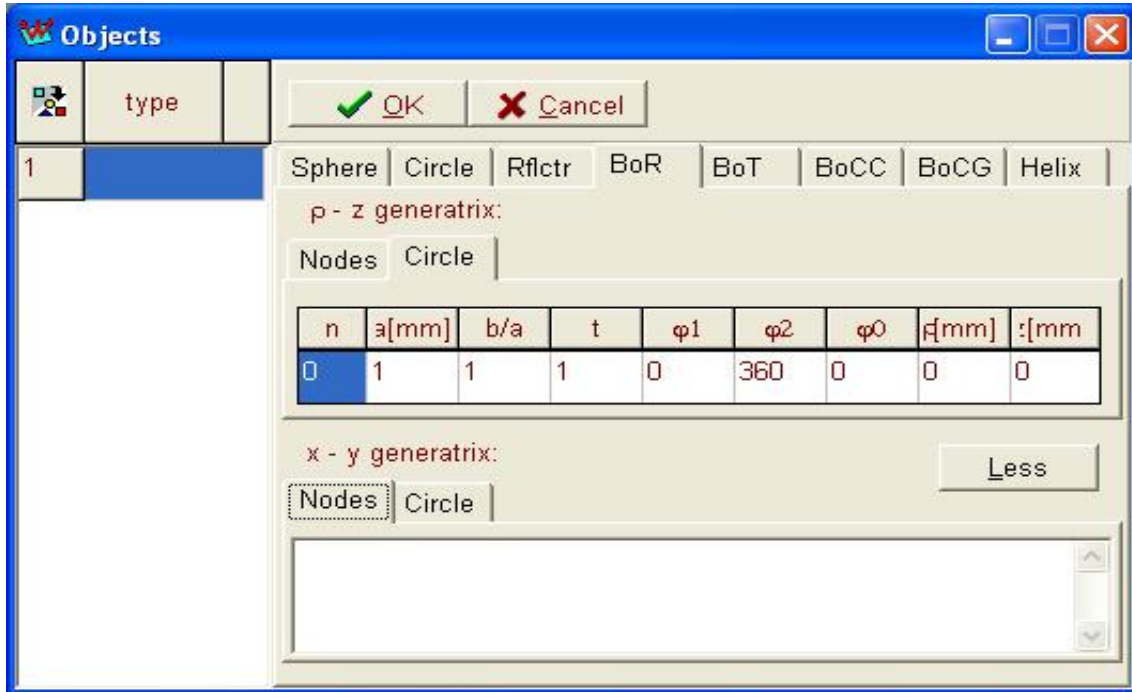
Fig. shows the object editor for placing BoR

The BoR page in the Objects editor has two forms as shown above. Click the button More to change the first form to the second one, and the button Less to go back.

Reflector:

Reflector object represents the geometrical model of a generalized reflector. Generalized reflector is a part of a generic surface, whose main axis coincides with the z-axis.

$$z = \rho^2/(4f) \qquad \rho^2 = x^2 + y^2 \qquad d/a - \text{paraboloidal}$$
$$z = d^2\sqrt{\{1 + \frac{\rho^2}{(f^2 - d^2)}\}}$$

If $(d/a)(a/f) > 1$ – ellipsoidal

$(d/a)(a/f) < 1$ – hyperboloid

where " f " is the focal distance (i.e. distance from the focus to the origin) and "d" is the minimal distance from the generic surface to the xOy plane. The aperture is bounded by a super quadric function defined by the equation:

$$\left(\frac{x-x_o}{a}\right)^{\frac{2}{t}} + \left(\frac{y-y_o}{b}\right)^{\frac{2}{t}} = 1$$

x_o and y_o define the aperture centre. When x_o and y_o are equal to zero the reflector is symmetrical, otherwise, it is offset. Factors a and b are the semi major and semi minor axes of the aperture and t is the shape factor. The shape and size of a generalized reflector are given by the parameters: a (mm), b/a, a/f, d/a, x_o, y_o, and the shape factor. In addition we can choose: **n** - number of segments per quarter of the circumference, **Part factor** – part of the generalized reflector (whole, half, quarter, 1/8), **Mesh type** – classic or other advance.

BoT (Body of Translation):

BoT represents the geometrical model of the body of translation. The BoT is obtained when the piecewise linear generatrix, placed in the yOz-plane, is successively shifted for segments of second piecewise linear generatrix, placed in the xOy–plane.
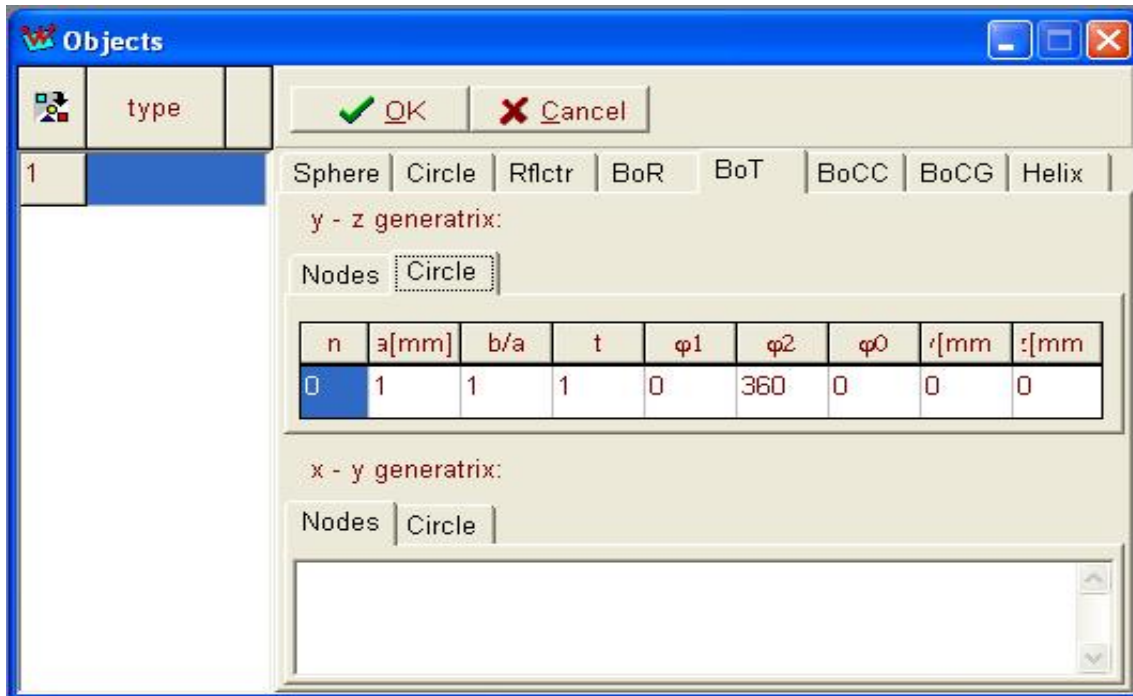
Fig. shows the object editor for placing the BoT

The first generatrix can be scaled after each shift.

BoCC (Body of Constant Cut):

The BoCC represents the geometrical model of the body of constant cut. The BoCC is obtained when the 1st piecewise linear generatrix is moved along

the 2nd piecewise linear generatrix, placed in the xOy plane, in such a manner that the body have the same cut in planes that are normal to the 2nd generatrix.
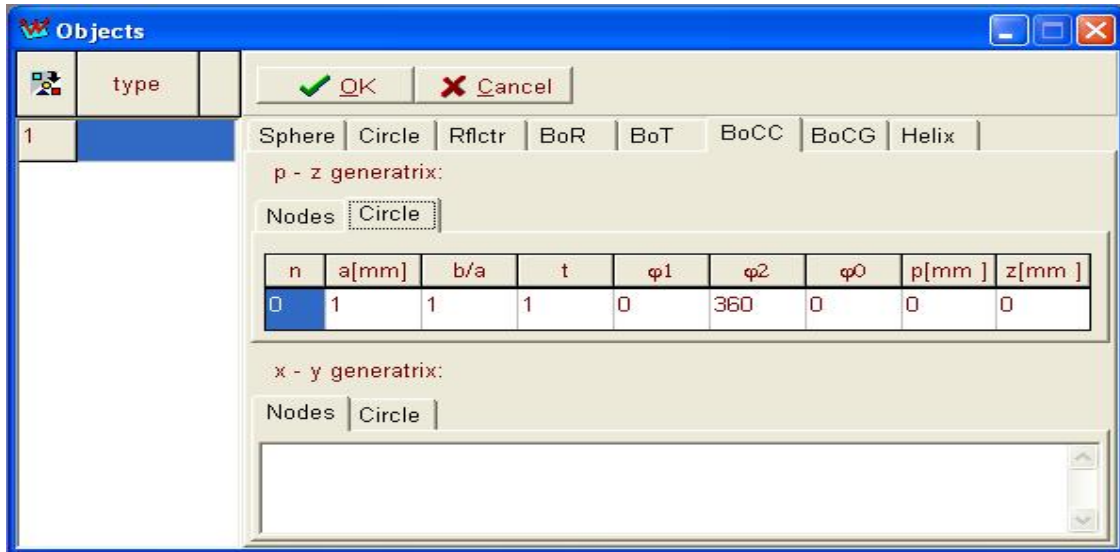
Fig. shows the object editor for placing the BoCC

The 1st generatrix is placed in the ρOz plane where the ρ axis remains normal to the xOy plane and it can be brought to the 2nd generatrix being zero.

BoCG (Body of Connected Generatrices):

The BoCG represents the geometrical model of the body of connected generatrices.
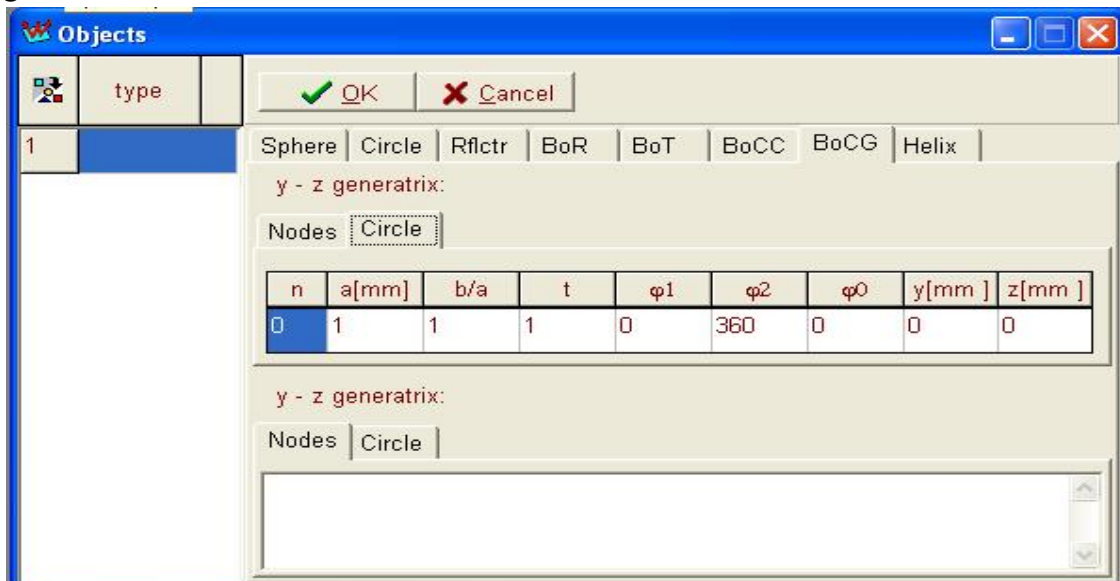
Fig. shows the object editor for placing BoCG

The BoCG is obtained when the 1st piecewise generatrix, placed in the yOz plane, is connected to the 2nd piecewise linear generatrix, also placed in the yOz-plane.

Nodes and Circle Generatrix:

Node generatrix represents an arbitrary piecewise linear generatrix in a plane defined by a sequence of at least two nodes. Nodes are given with two coordinates. First nodes represent the starting coordinate and the last node represents the end coordinate. The node window:
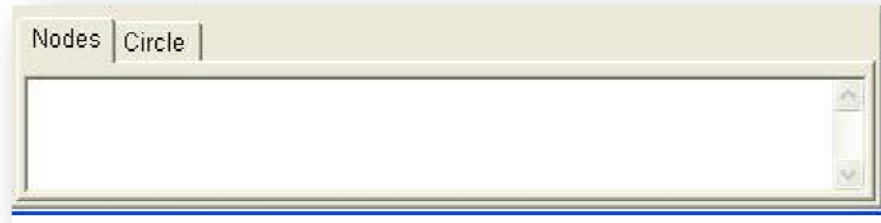
Fig. shows the block of defining the node

Circle generatrix represents a piecewise linear approximation of a super quadric function or its part, which can arbitrarily located and oriented in a plane. The shape and size of an original generalized sphere are given by the parameters: a, a/b, and t ; in addition we have:

Fig. shows the block of defining the circle

- n – number of segments per quarter of the ciccumference,
- φ_1 – start angle,
- φ_2 – stop angle,
- φ_o – rotation angle,
- ρ – shift along the xOy plane,
- z – shift along the z-axis.

Helix:

A helix object represents the geometrical model of a helicoidally antenna which can be composed of the following: wire/plate, with/without dielectric

core, unifilar/duofilar/trifilar/quadrifilar, linear/exponential, cylindrical/conical/ spiral shape, single/multiple and so on.
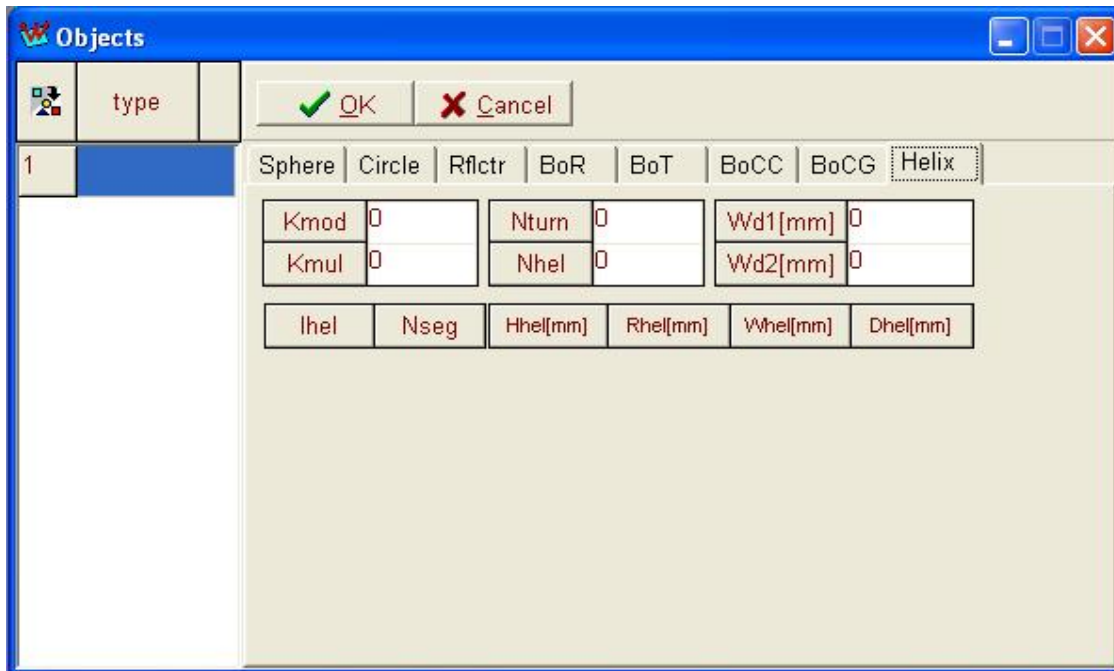
Fig shows the object editor for placing helical structure

List of parameters:

- Kmod – type of building elements: while Kmod =1 then the helix is mzde up of wire and always of pure metal, again when Kmod = 2 then the structure is made up of plates.
- Kmul- multiplication constant (1 – unifilar, 2 – duofilar, 3 – trifilar, 4 – quadrifilar etc.)
- Nturn – number of segments per one turn. (must be multiple of Kmul).
- Nhel – total no. of interconnected helices.
- Wd1 (Wd2) – distance from the beginning (end) of multiple helix axes from bottom (top) of the dielectric rod.
- Ihel – types of helices (1 – linear, 2 - exponential).
- Nseg – number of segments of helices.
- Hhel – z coordinates of the helix.
- Rhel – radial coordinates of the helix.
- Whel – radii of the wire helices.

MANIPULATION:

The Manipulations editor as listed performed the various manipulation with previously created entities. Each row of Manipulations list defines one manipulation. When a new project is created, the list is empty and the manipulation descriptor is not visible. When the first row in the Manipulation list is inserted by dragging the generic icon the Manipulations descriptor becomes visible. Each of the six Manipulate pages defines a specific type of manipulation:
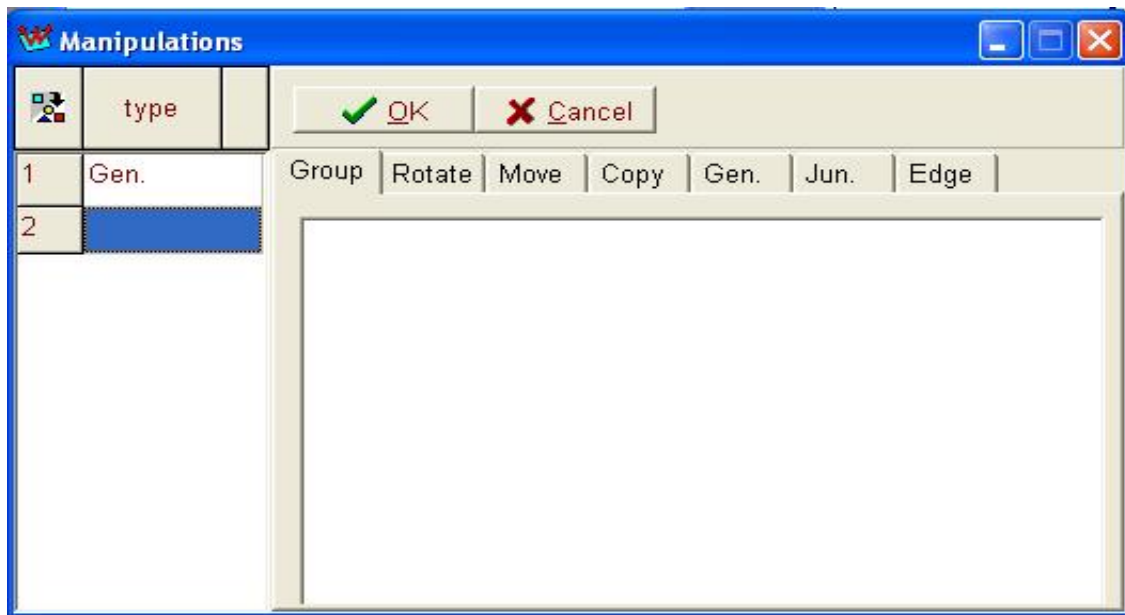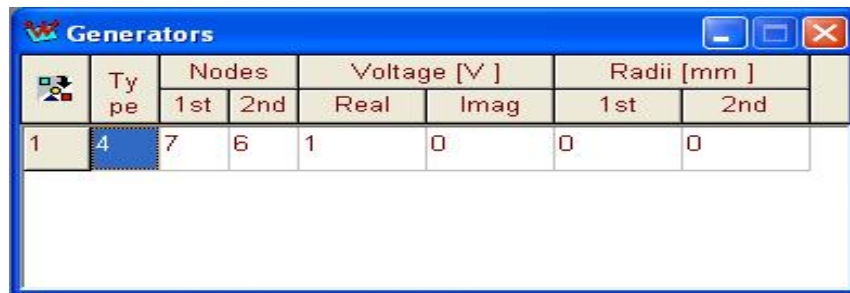
Fig shows the Manipulations editor page for doing manipulation

- Group – Specifies which entities (wires, plates, objects and groups) should treated as a single entity that can be further grouped, rotated, moved and copied.
- Rotate – Rotates the entities about the x, y, z-axis.
- Move – Shifts entities along the x, y, z-axis.
- Copy - Copies the specified entity, one or more times. Each copy is obtained by rotating, moving, and scaling the previous copy. If the no. of copies is zero, the original is rotated, moved, and scaled.
- Gen – Changes voltages of existing generators after the complete structure is created by using the Object and/or the Manipulation editor.
- Jun – Defines non-trivial junctions after the complete structure is created by using the Object or Manipulation editor.
- Edge – Defines edging at plate to dielectric surface junction.

GENERATORS:

After the modelling of the antenna is finished it is required to give the feeding at the desired position. For this, the software provides the facility of placing generators. The generator is always connected to one of a wire, and its reference direction is towards another node of the wire. A generator is completely determined by these two nodes and complex voltage across them. The nodes associated with the generator are specified by their order no. given in the Nodes table. The generator table can be opened from the excitation menu.

Fig shows the generator editor page for placing generator
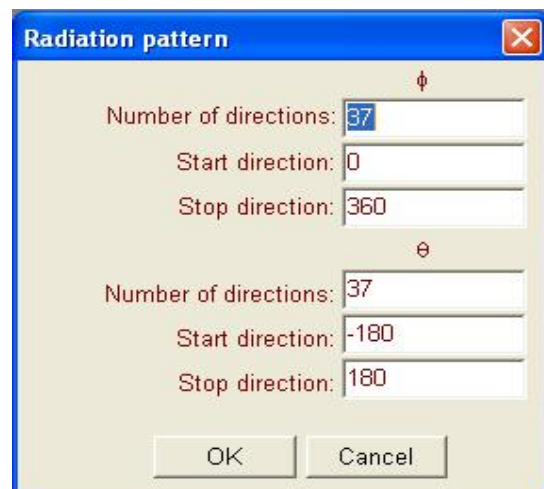
If there lays more than one generator then we can select the operation mode of the generator to be one at a time, or all the generators at a time as desired.

SPECIFYING THE OUTPUT RESULTS:

Calculation of the output results is performed by using the options Current, Radiation and Near-Field, from the output result menu.

Far field is computed at one or more uniformly spaced angular directions. These specify to the angular direction by the spherical Φ and θ coordinates. The Φ coordinates is measured from the x axis in the xOy plane. The θ coordinate is measured from the xOy plane to the z-axis. Hence it is the elevation angle. The spaced angle range is completely determined by the number of directions along the Φ-coordinate, the start and stop angles of Φ, and the number of directions along the θ-coordinate, and the start and stop angles of θ.

Fig shows the page for the radiation pattern

The near–field is the calculation for the complex electric field and the magnetic field at a specified set of uniformly space grid points. The desired frequency at which the output result should start and the stop frequency must be given from the options frequency in the Edit menu.

Fig shows the page for the near-field pattern:
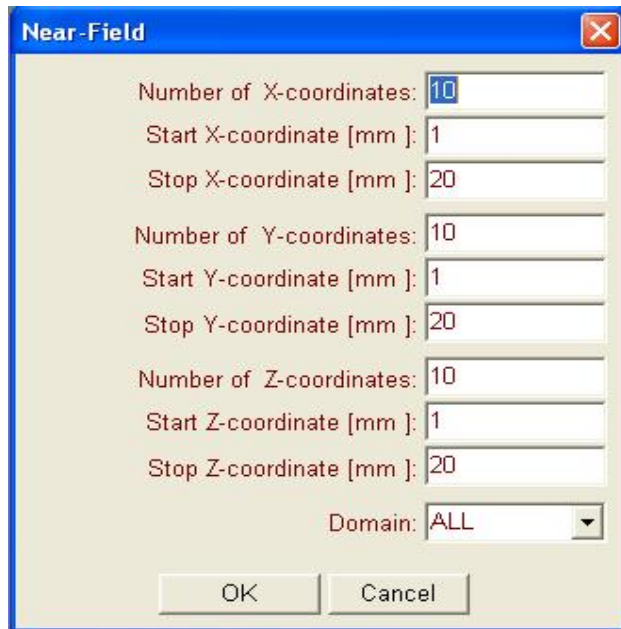
RUN ANALYSIS:

As soon as the parameters are set properly the model is ready for the analysis. The running time of the analysis depends on the input data and the hardware of the computer. It can be done by selecting Run from the Run menu, the run screen appears and the analysis is started.
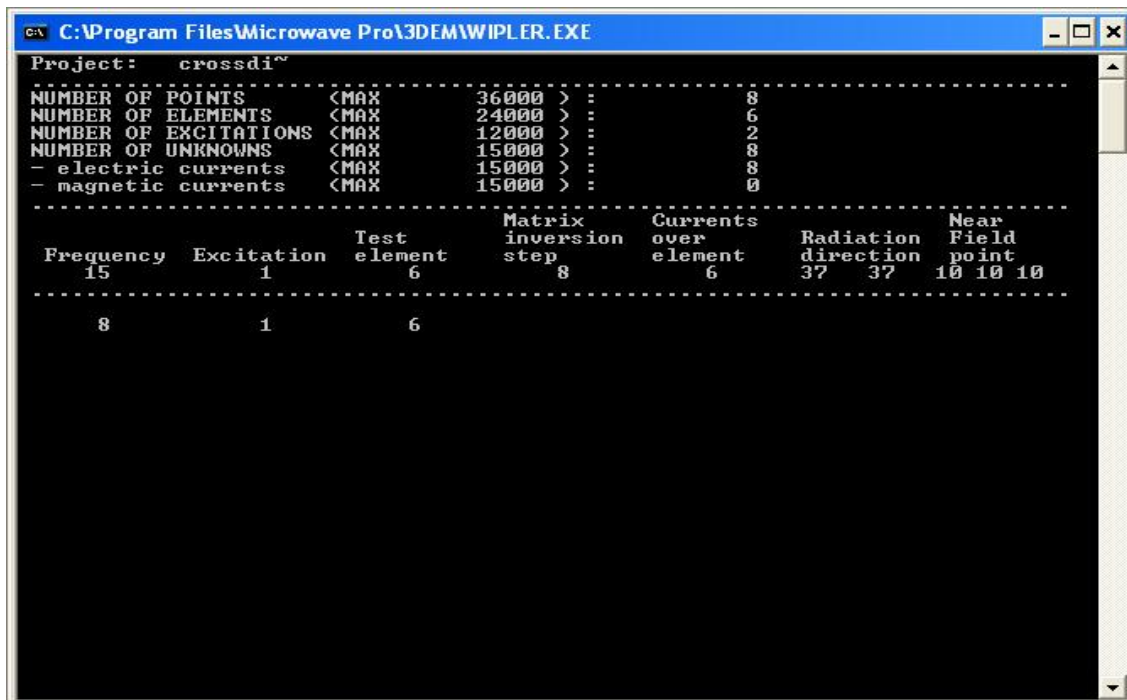
Fig shows the run screen

Plotting the Results:

Lastly we can plot the results of our model. WIPL-D provides to see the admittance parameter, impedance parameter and the scattering parameter. The radiation pattern in 3D as well as 2D can be viewed which can be also viewed in Spherical or Cartesian coordinates. To see the results select Graph option in the Output menu.
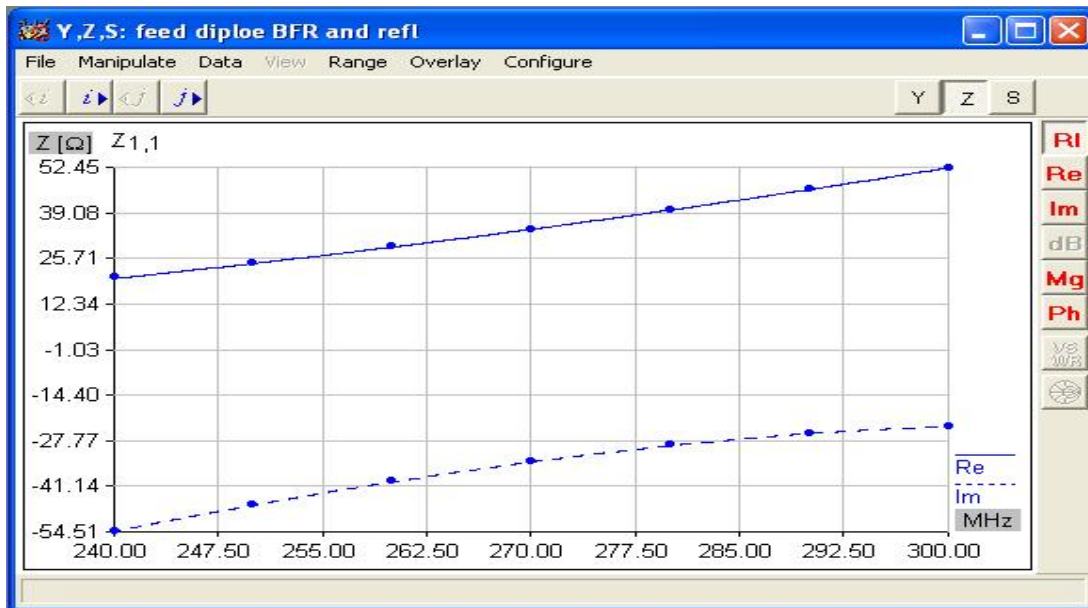
Fig shows the output impedance parameters
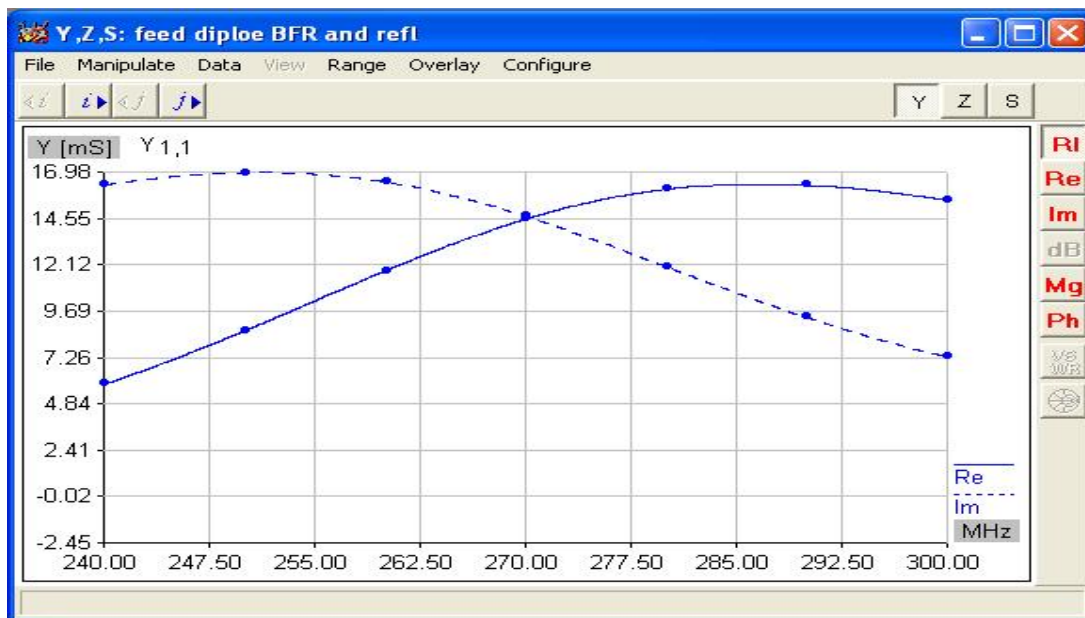
Fig shows the output impedance parameters
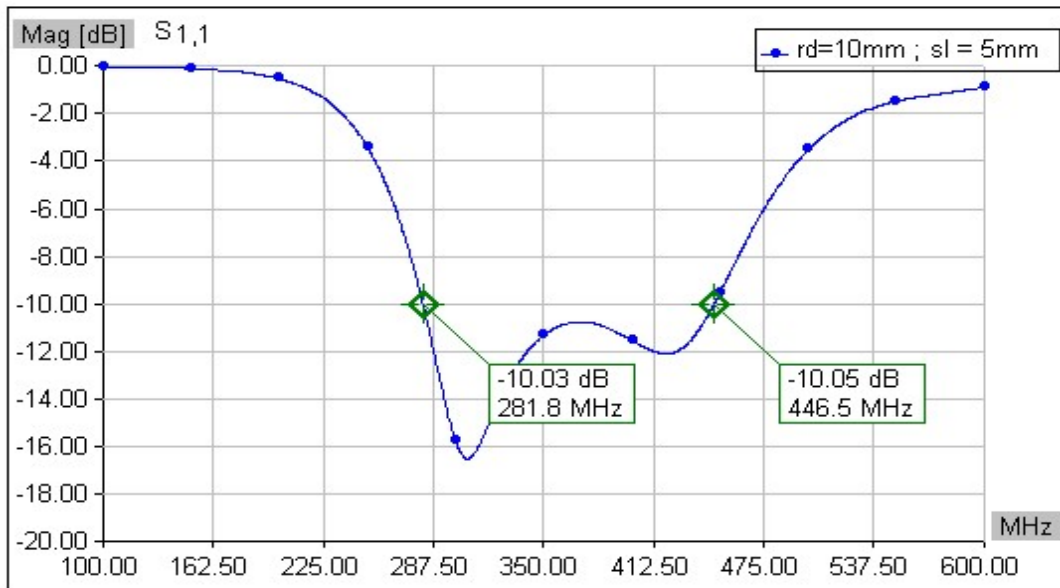
Fig shows the S parameter output result
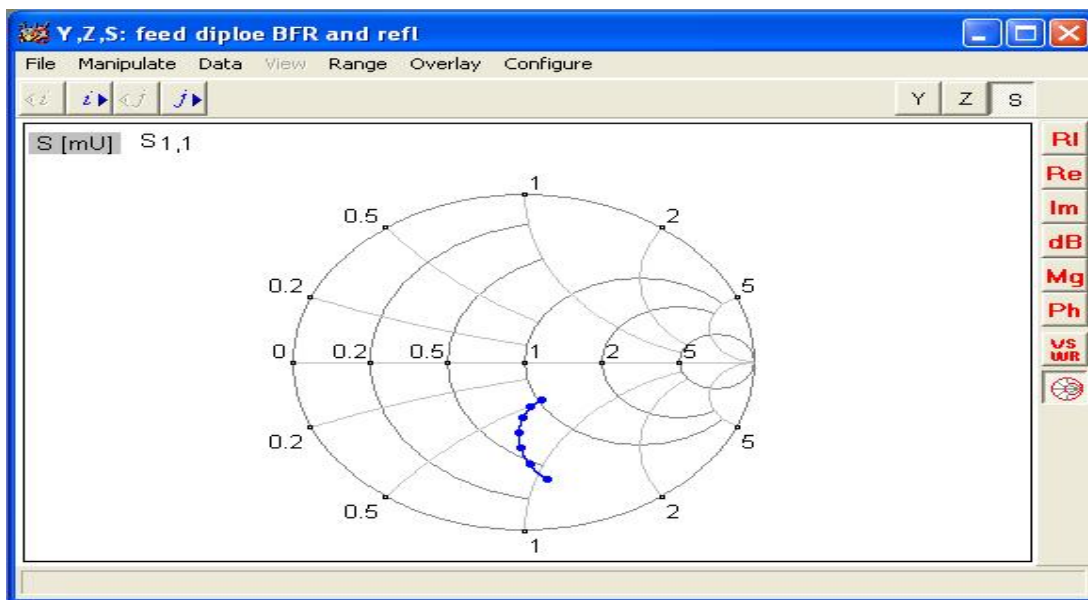
Fig shows the Smith chart of a designed model

The above fig shows some of the output windows which are provided by the software.

Testing of the Software (WIPL-D):

As required, before the use of the software for further designing and simulation purpose on new ideas it is necessary to test the software in order to know about its accuracy of giving output and its perfection. So, since the software is newly introduced the first step that is done is to study the software about its features and etc. To test the perfection/accuracy about its output we worked on the characterization of the 327 MHz feed that already exist there, we see the radiation pattern of the feed both from the software (we consider as theoretical) and practically obtained readings got matched up to an appreciable level. This work is completed in the following steps:

Geometrical model of the feed:

As the name of the software termed as 3D EM Solver, first the modelling of the desired feed should be done in the 3D plane, hence we started with the same. Below shows the geometry of the 327 MHz feed which is a cross dipole:
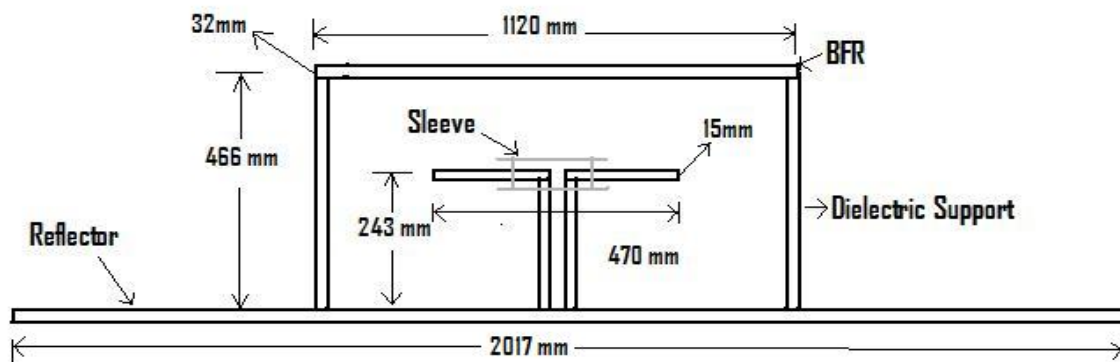
It consist of a cross dipole covering with the sleeves (the geometry is shown aside) above the dipole lies the beam forming ring (BFR) parallel to the reflector (mesh) that lies below the dipole.
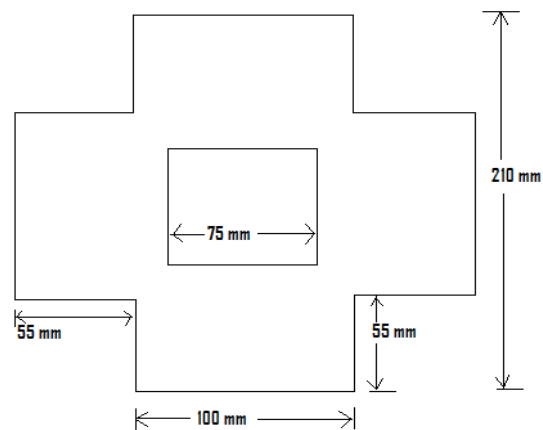
Fig. The 327 Mhz feed and the Sleeve geometry

Designing with the Software:

The nodes are defined in the 3D plane with respect to the given measurement of the feed, then for the dipoles (maintaining the feeding gap to be 42 mm) we had the wires and placed the generators as required. The structure is shown below:
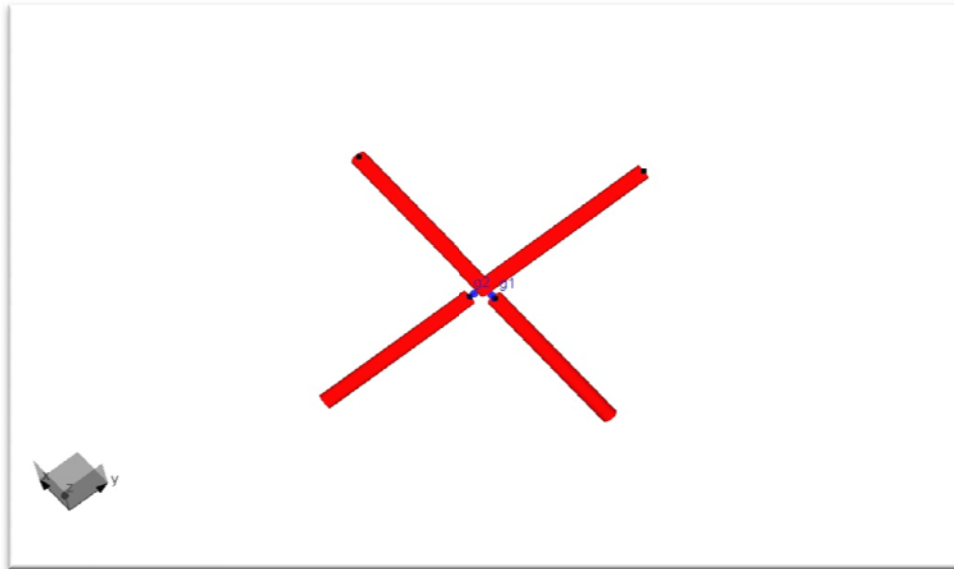
Fig shows the cross dipole with the generators (g1 & g2).

Then comes the placing of the plates covering the dipole (which were mainly used for increasing the band width) as shown,
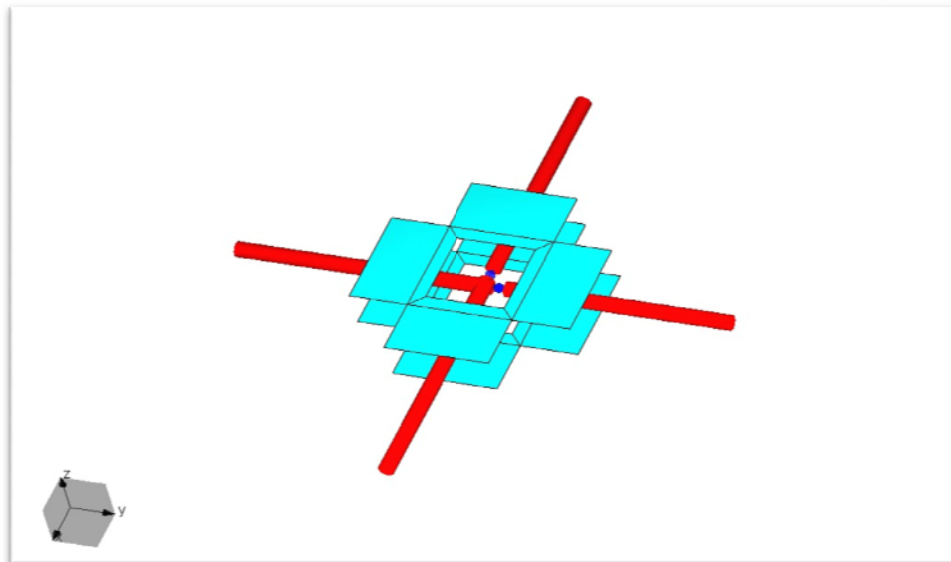
Fig. Dipoles with the sleeves.

With the Object editor page BoR (Body of Revolution) we placed the "beam forming ring" (BFR) above the dipole;
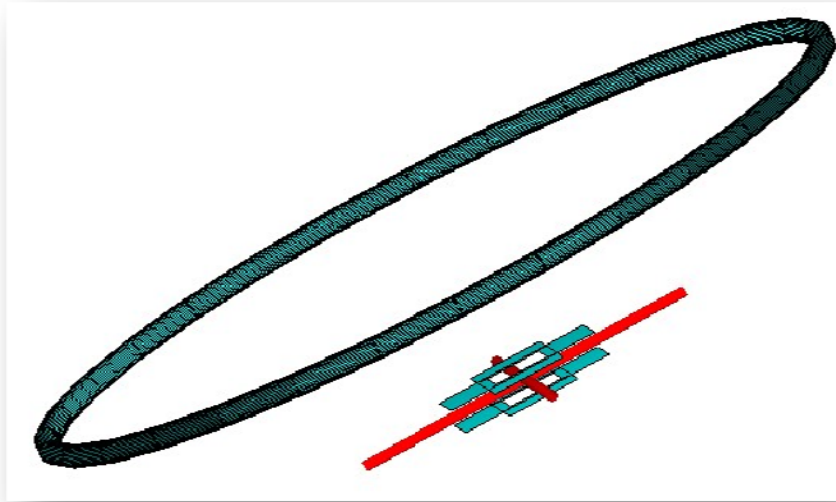
Fig BFR placed above the dipoles.

Again with the Object editor page we placed the reflector below the dipole at the given distance:
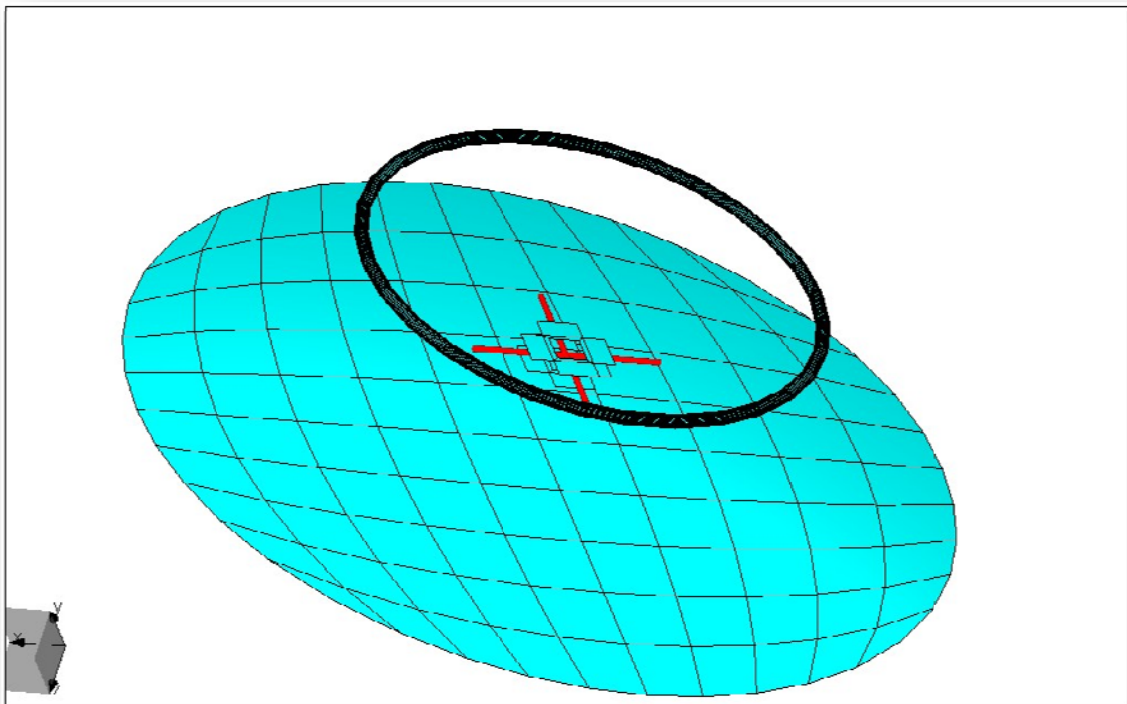
Fig. overall 327 MHz feed.

Mainly we are interested in the far field radiation pattern of the E and H plane, after the simulation we found some of the graphs as follows:
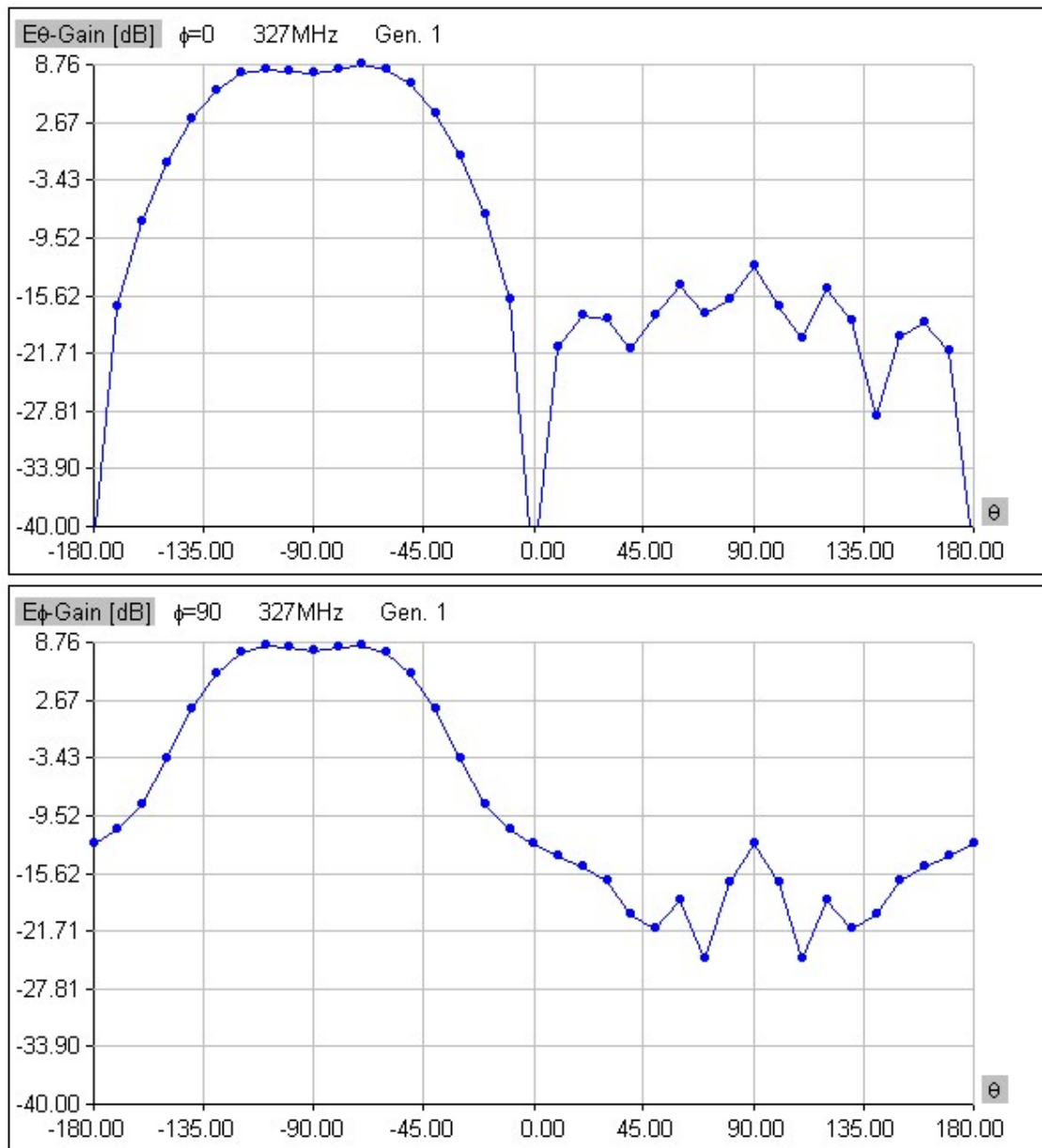
Fig shows the E plane and the H plane respectively

Here the back lobe gets reflected due to the presence of the reflector and an additional gain is achieved at the front lobe. But in order to get matched with the practical reference we made transformation of angle θ from 0° to 90°. Then we had the following combined plot of the E and H plane at the frequency of 327 MHz:
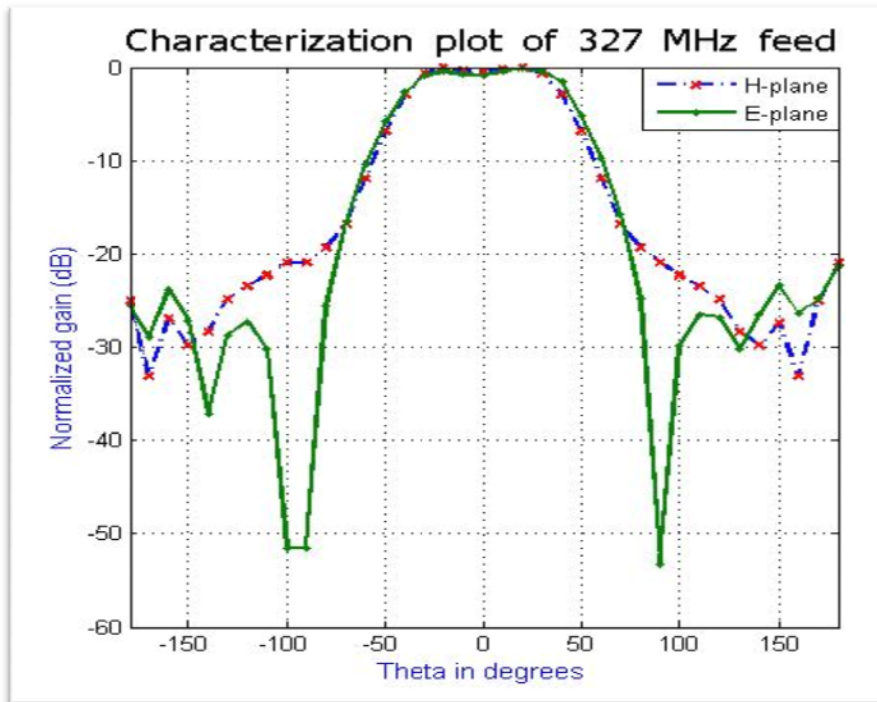
Fig E and H plane for the 327 MHz feed (Simulated)

Comparison of the E and H planes, achieved through the software simulation and the practically measured values were observed by overlaying both the observation data:
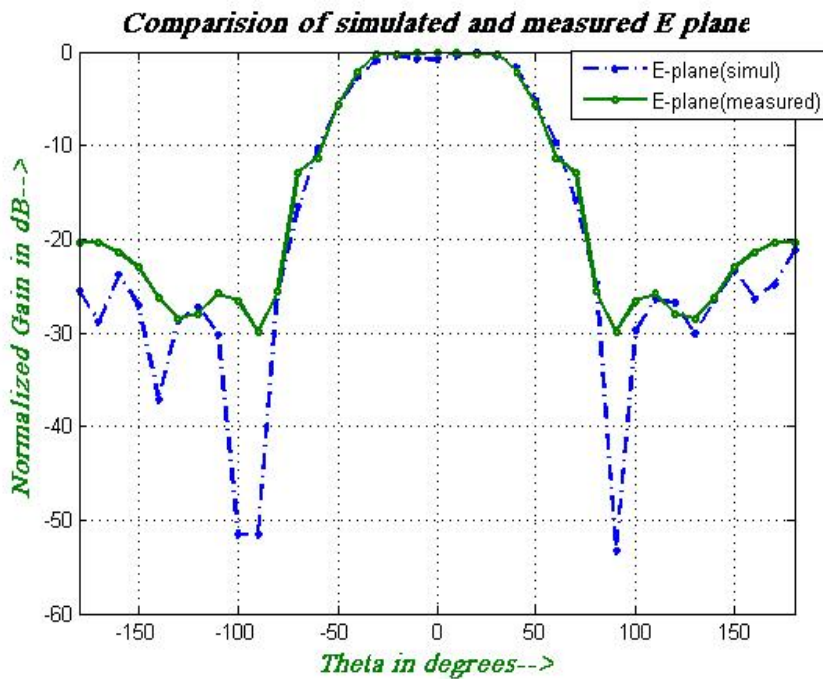
Fig Comparison of the simulated and practically measured E planes
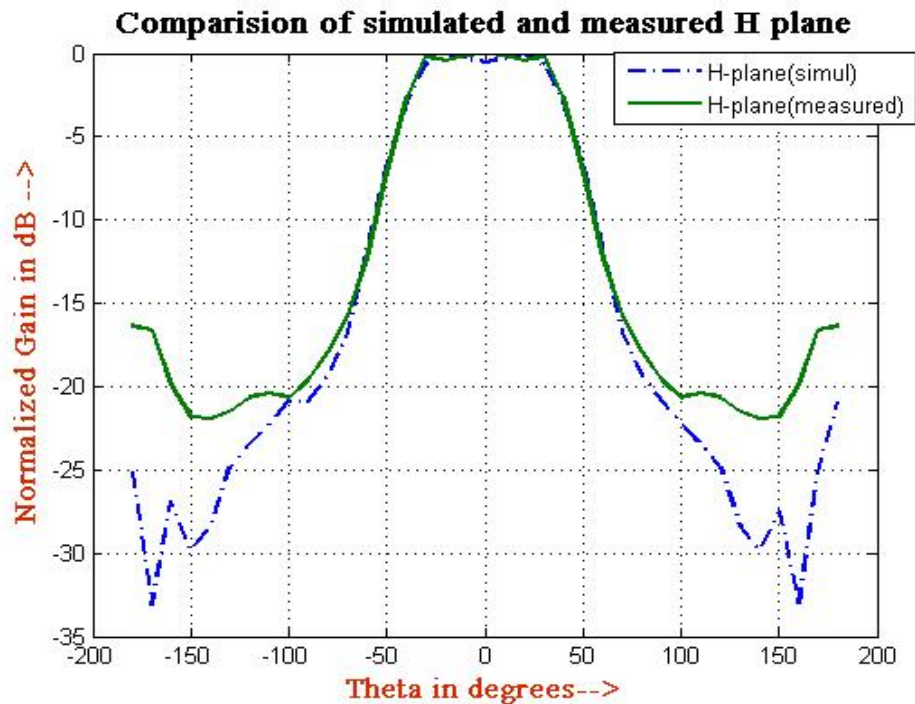
Fig Comparison of the simulated and practically measured H planes

From the comparisons we can see that both E and the H planes are matching up to an appreciable position. The other parameter such as SWR and the scattering parameters also give a good output and slightly deviate as it's too ideal.

With this the testing of the software completes.

Further testing with the BFR position:

The BFR i.e. the "beam forming ring" is placed above the dipole parallel to it and the reflector as shown, only to suppress the H plane so that it get matched with E plane and hence reducing the chance of getting undesired polarization.

A matched E and H plane is achieved due to the beam forming ring which suppressed the H plane without affecting the E plane, some of the radiation pattern are observed by changing the height of the BFR distance above the dipole. The BFR height is change within 10mm on either side and H plane change slightly, in one case it goes off the E plane earlier and in the other case the H plane gets more compressed than earlier. The graphs are shown by the next:
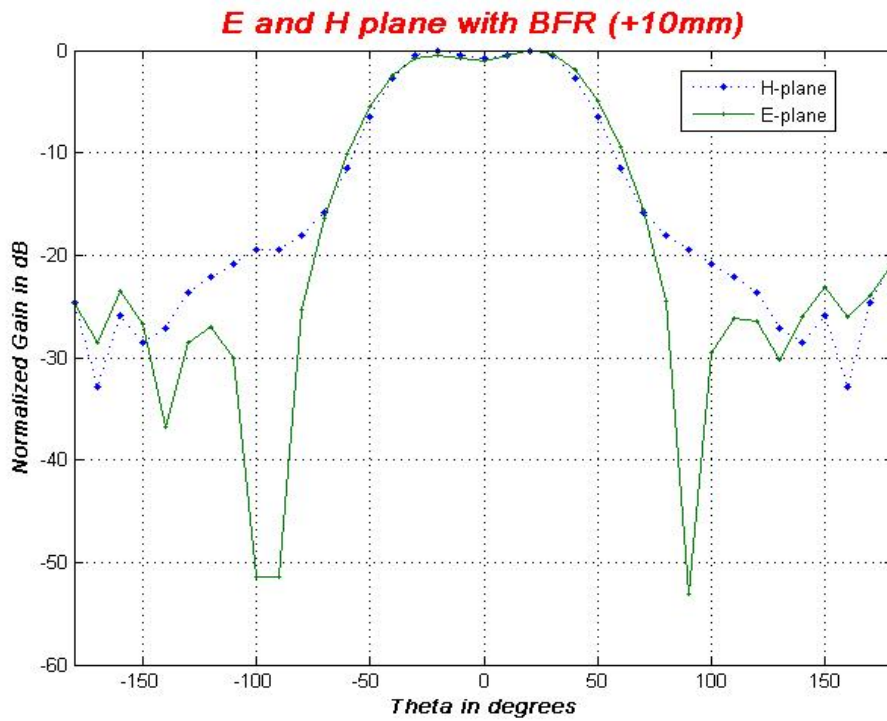
Fig BFR placed 10mm above than the actual position
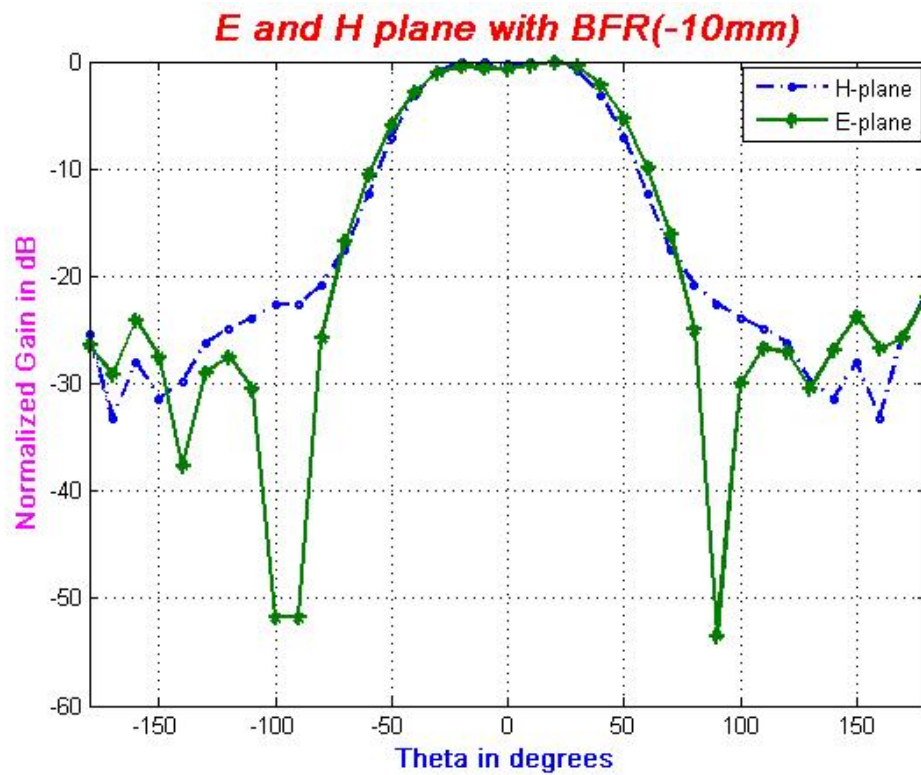
Fig BFR placed 10mm below the actual position

Increasing the Operational Bandwidth:

A very thin dipole has of course a narrow bandwidth characteristic since it owns a narrowband input impedance characteristics. The operational bandwidth can be increased or enlarged is by decreasing the *l/d* ratio. For a given antenna, this can be accomplished by holding the length the same and increasing the diameter of the wire. Here also we tried to increase the operational bandwidth of our dipole by changing (increasing) its diameter, also, as the sleeve plays an important effect on the bandwidth we tried to change its distance from the dipole and the following results were obtained:
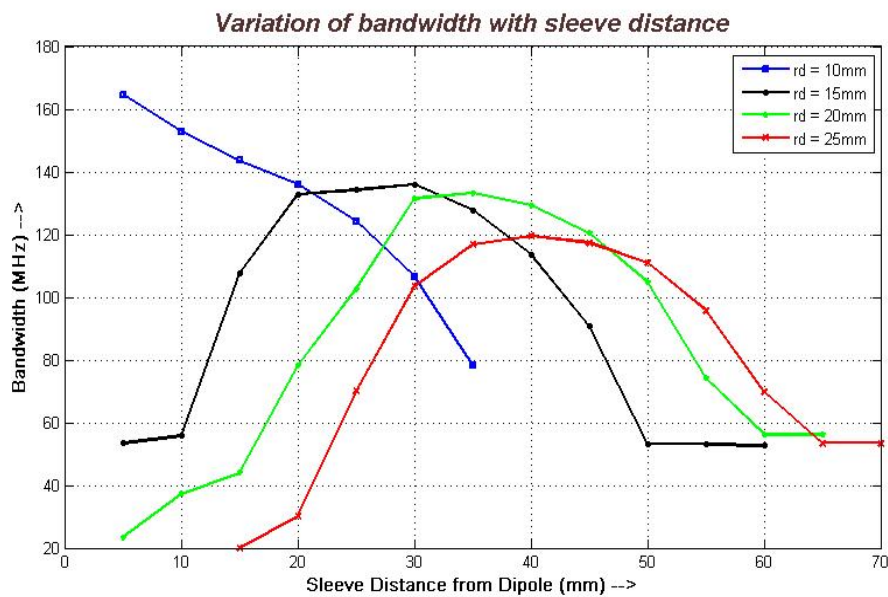
Fig shows the variation of BW w.r.t. the sleeve distance of certain dipole radius
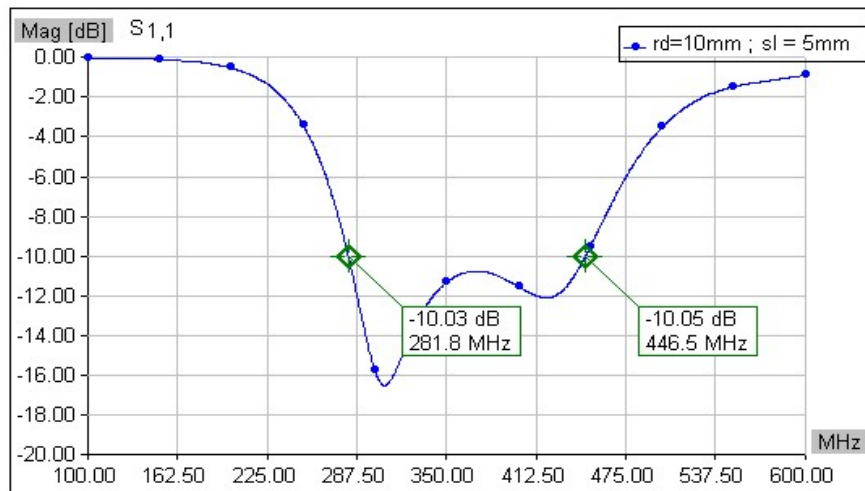
Fig s11 output of the dipole rd=10mm and sleeve distance =5mm

We take the band width in terms of return loss parameter S_{11} at -10 dB cut of point since at this point the Standing Wave Ratio (SWR) of the system is < 2, which is the required condition for having low reflection coming back. The graph shows the operational bandwidth of the cross dipole of various diameter and the sleeve placed at different distance. In the plot "*rd*" represents the dipole radius in mm and with the variation of the sleeve distance due to change in the capacitive effect the input impedance characteristics change and hence the bandwidth.

The First Version of a Prototype Feed:

From the graph we take our next model of the feed to be cross dipole of radius **10 mm** and sleeves are maintained at a distance of **5 mm** from the dipole which gives us a bandwidth of around **162MHz**.We keep all the other configuration the same as that of earlier and observed the radiation pattern i.e. the E and H plane:
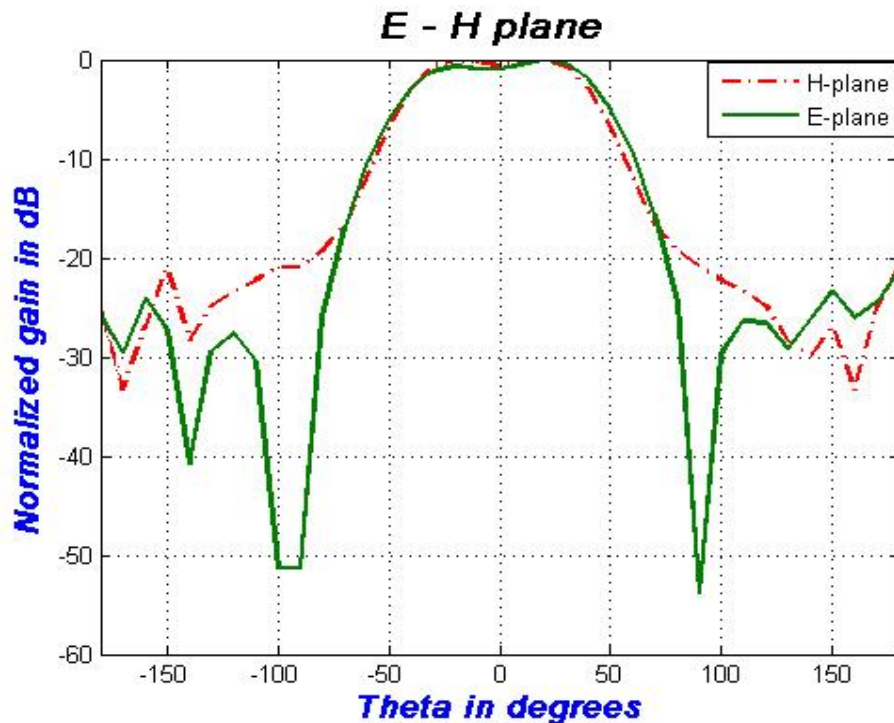
Fig shows the E – H plane of the new dipole with rd=10mm and sleeve distance =5mm

Next, using Matlab, the beam width measurement of the E and H plane was done at different frequencies at -3 dB and at -6 dB cut off point and circularity (variation of the ratio of the E plane to the H plane with respect to the frequency) is observed. The following observations were found:
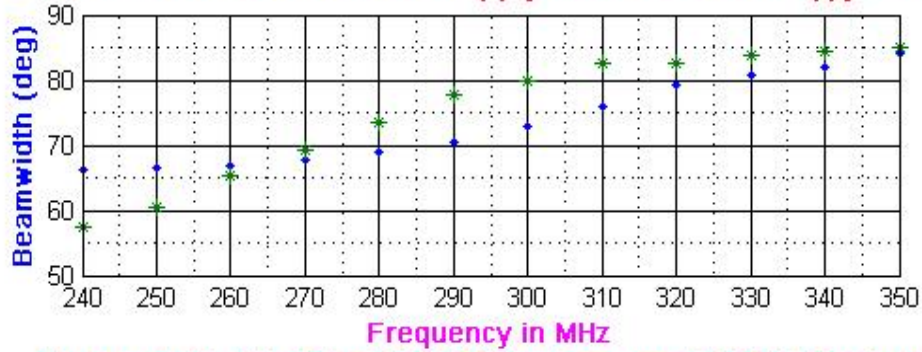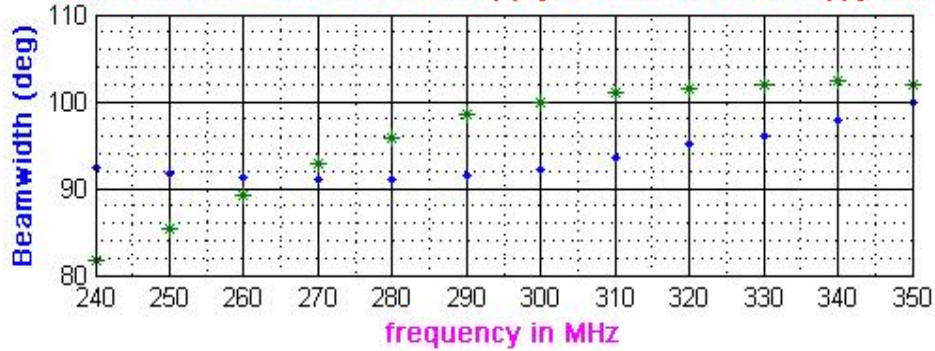
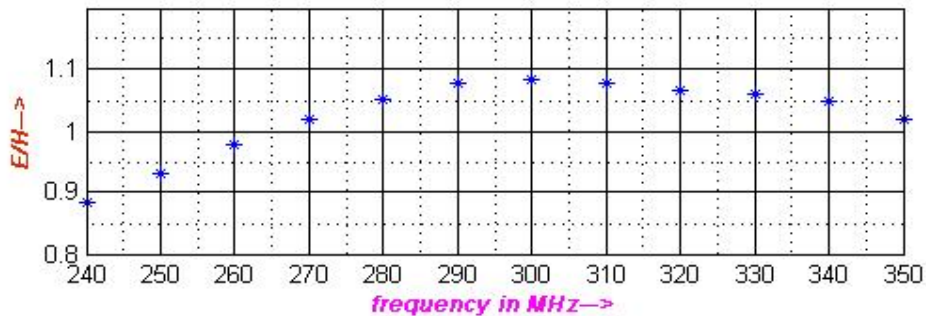Fig shows the beam-width variation at different frequencies
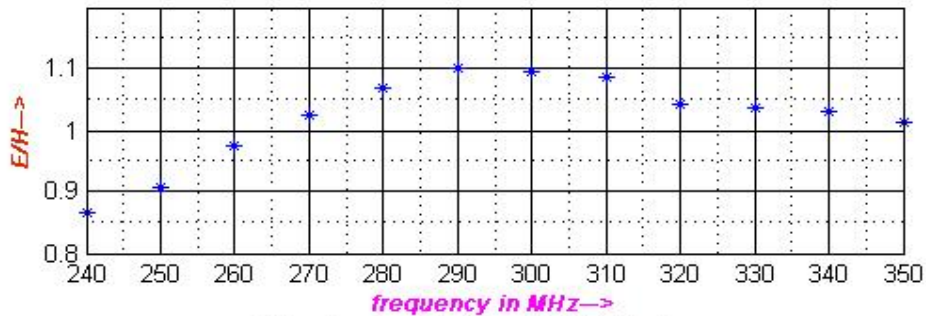
Fig shows the circularity plot at different frequencies

We again tried to see radiation pattern of the modified dipole by changing the tube diameter of the BFR, as well as the ring diameter which shows some change in the H plane but not in the E plane. The patterns obtained with their respective variation are given next:
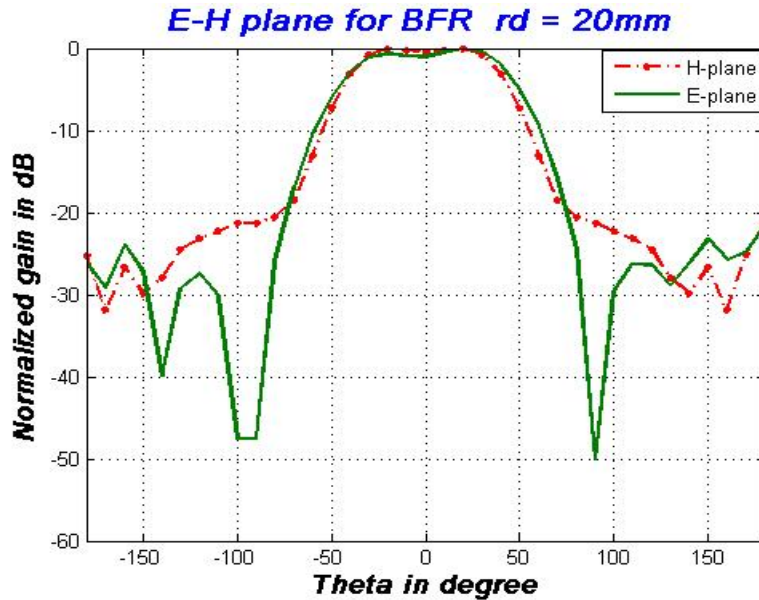

Fig E – H plane for the BFR tube radius = 20mm

Earlier the BFR tube radius was 16mm; here we observed the radiation pattern by increasing the tube radius to 20mm. From the graph above it can be seen that the H plane is slightly compressed more than the earlier case.
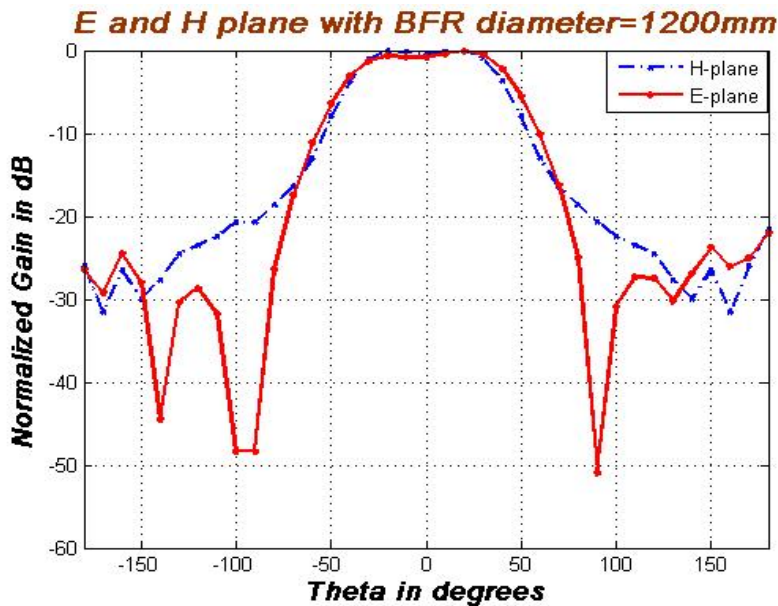

Fig E – H plane for the BFR ring diameter = 1200mm

The ring diameter is increased to 1200mm and the H plane goes off earlier than the previous observation.

Next we see the current distribution over the dipoles after simulation it comes out as shown below:
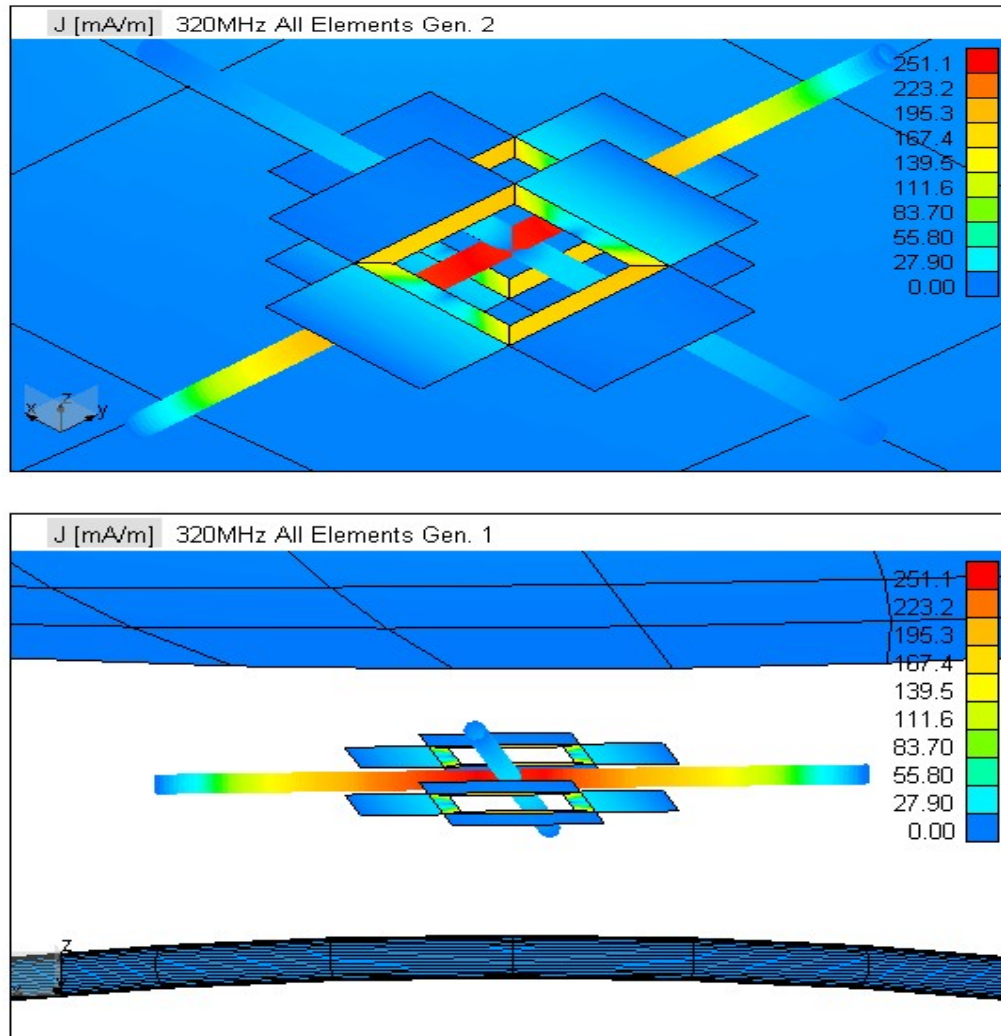

Fig shows the distribution of the current over the dipoles

The current is maximum (loop) at the centre and nearly equal to zero (node) at the end point. The current actually doesn't reach zero at its node because of the end effect which comes due to the RF resistance of the wire (ohmic resistance) and the radiation resistance. The ohmic resistance of a half wavelength antenna is ordinarily small enough compared with the radiation resistance, to be neglected for all practical purpose. In this software the current distribution is mainly measured in mA/m and the values are shown besides in the figure itself.

An approach to the BFR concept:

It is an amazing fact that BFR i.e. the beam forming ring only suppressed the H plane leaves no significant change on the E plane. May this effect be visualized from the loop which is sensitive to the magnetic field and very less to electric field?

The loop follows the Faraday's law of induction which states that the induced electromotive force *e(t)* in a loop is directly proportional to the time rate of change of magnetic flux *Φ(t)* through the loop. Can it be used to explain the effect of the BFR for the suppression of the H plane?

Again drawing our attention to the fact that it occurs only with a circular loop but not with a square loop, this we try to see the radiation effect by making two geometrical model of a circular like and a square loop of equal area with the tube diameter of 16mm separately. The two models are shown below:
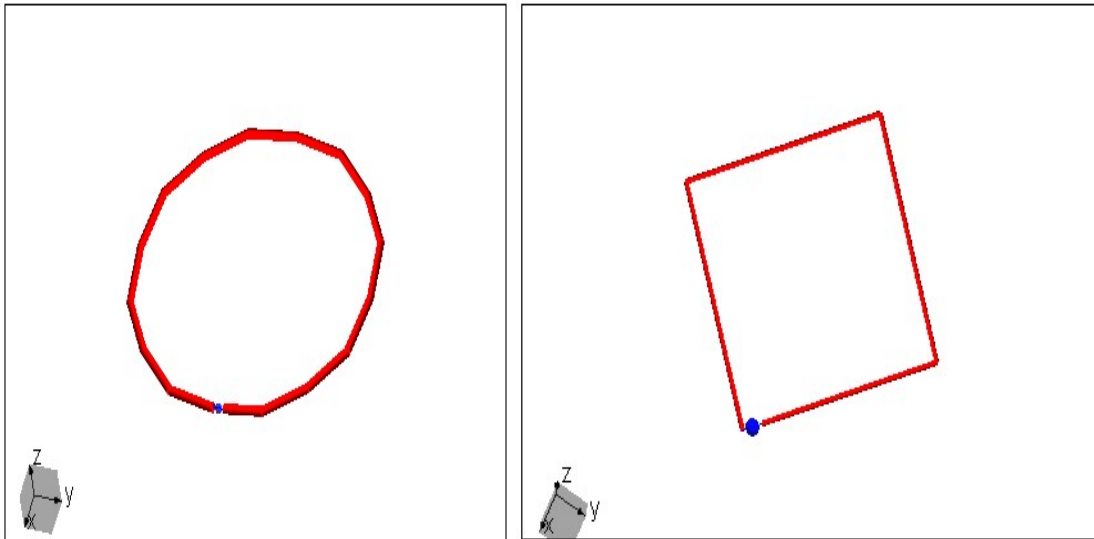

Fig the two models taken to be as BFR

The radiation pattern is observed as that we observed for the H plane in case of the dipole. The patterns are shown in the next page which may support the occurrence of the effect why the circular BFR. One should not get confused with the radiation pattern as the transformation of the angle θ from 0° to 90° is not done here as done in the case of the dipole for the matching with the practically measured reading. The pattern shows a good difference in the pattern at different angles of Φ, we observed the following at frequency 327 MHz and $Φ = 90^o$.
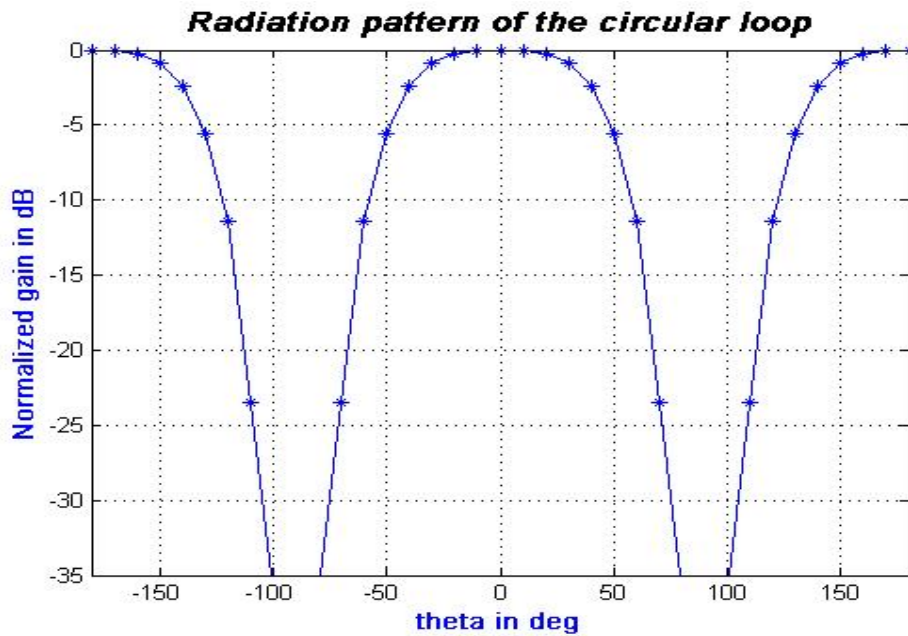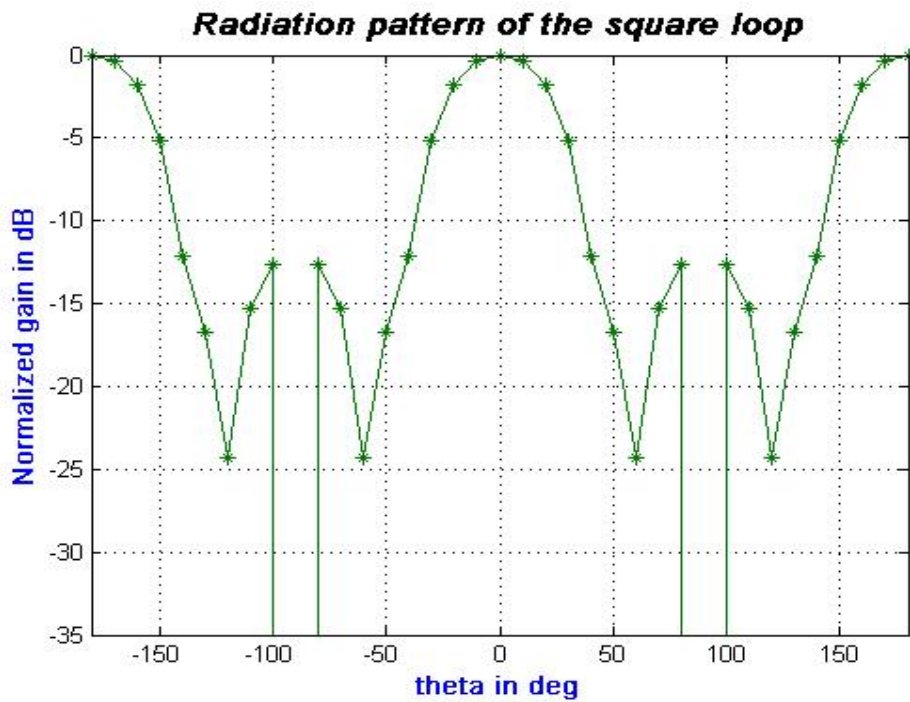
Fig shows the radiation pattern of the circular loop

Fig shows the radiation pattern of the square loop

The two patterns show clearly the difference of the two models and might it be a reason for the approach towards the concept of the BFR holding the root of the circular loop.

Conclusion and Further work to be done:

WIPL-D software is a user friendly program. The calculations are done in frequency domain. It enables us to define the geometry of any structure in any interactive way as a combination of wires, plates and material objects. As an output WIPL-D provides the current distribution on the structure, radiation pattern, near field distribution, admittance, and S-parameters at the predefined feed points. It also provides a variety of printer based and graphics output capabilities, including 2D and 3D graphs of the parameters of interest. Duration of the simulation time or time taken by the software to complete its run analysis may be of 3 seconds to several hours. It depends on the number of objects we are using in our model, lesser the number of objects, structures, lesser will be the time taken to complete the simulation, and also it depends on the number of frequencies needed between the start and stop frequency. Hence it is required to design the model of the antenna to an utmost perfection so that time may not waste.

In our work we designed the 327 MHz feed can see that the simulation results by the software matched appreciably with the practical readings. Thus we could proceed to imply and design new antenna structure.

As we desire for a larger operational bandwidth, from the software by changing the some of the parameters of the 327 MHz feed dipole design we obtained an operational bandwidth of almost 162 MHz the new dimensions are given as follows:

- Overall dipole length: 470 mm
- Diameter of the dipole: 20 mm
- Sleeve distance from the dipole on either side: 5 mm

The sleeve dimension is maintained at the same as earlier.

A practical implementation on the design will give the simulation purpose a complete shape to see whether both simulated and the practical observations are properly matching or not. Moreover in our design one can add the total 45m dish at the back and see the beam-width and the circularity plot.

For the requirement of larger operational bandwidth one can also see by varying the dipole length, one was found to be of 428 mm length which holds well and the band width varies much with the variation of the sleeve distance. Through this software one may also try to see the change regarding the BFR to put forward a proper explanation.
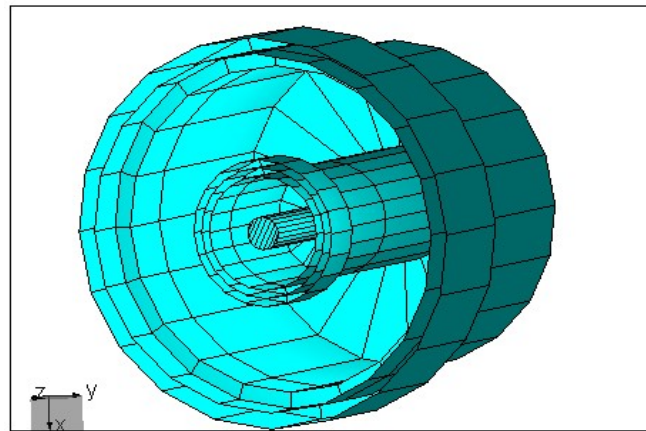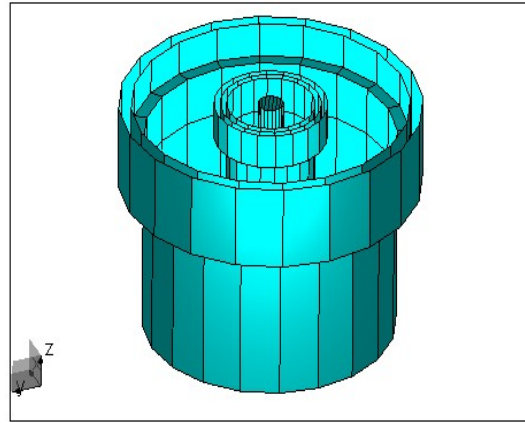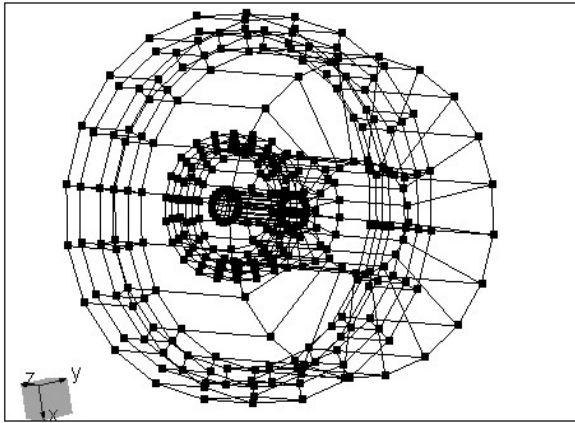
A model of the coaxial feed is viewed and is shown above. The coaxial feed has the capacity of receiving multiple bands of frequency, which are desired for astronomical observation. So with this software, one may try to design different coaxial models and its patterns of radiation, VSWR as provided by the software and implement it practically.

References:

- Antenna Theory Analysis and Design
                                    - by C. A. Balanis

- Electromagnetic Compatibility Handbook
                                    - by K. L. Kaiser

- The ARRL Handbook for Radio Armature

- Low Frequency Radio Astronomy
        Chapter 19: GMRT Antennas and Feeds
                                    - by G. Sankar

- WIPL-D Pro User's Manual

- Analysis of NCRA/TIFR GMRT 45m Dish Performance at 327MHz
                                    - by T. Krishnan

- Matlab Programming